

AD-A058 567

SOUTHWEST RESEARCH INST SAN ANTONIO TEX
DEGRADATION STUDIES OF A DI(2-ETHYLHEXYL) ADIPATE LUBRICANT BAS--ETC(U)
JUN 78 J P CUELLAR

F/G 11/8

F33615-76-C-2020

UNCLASSIFIED

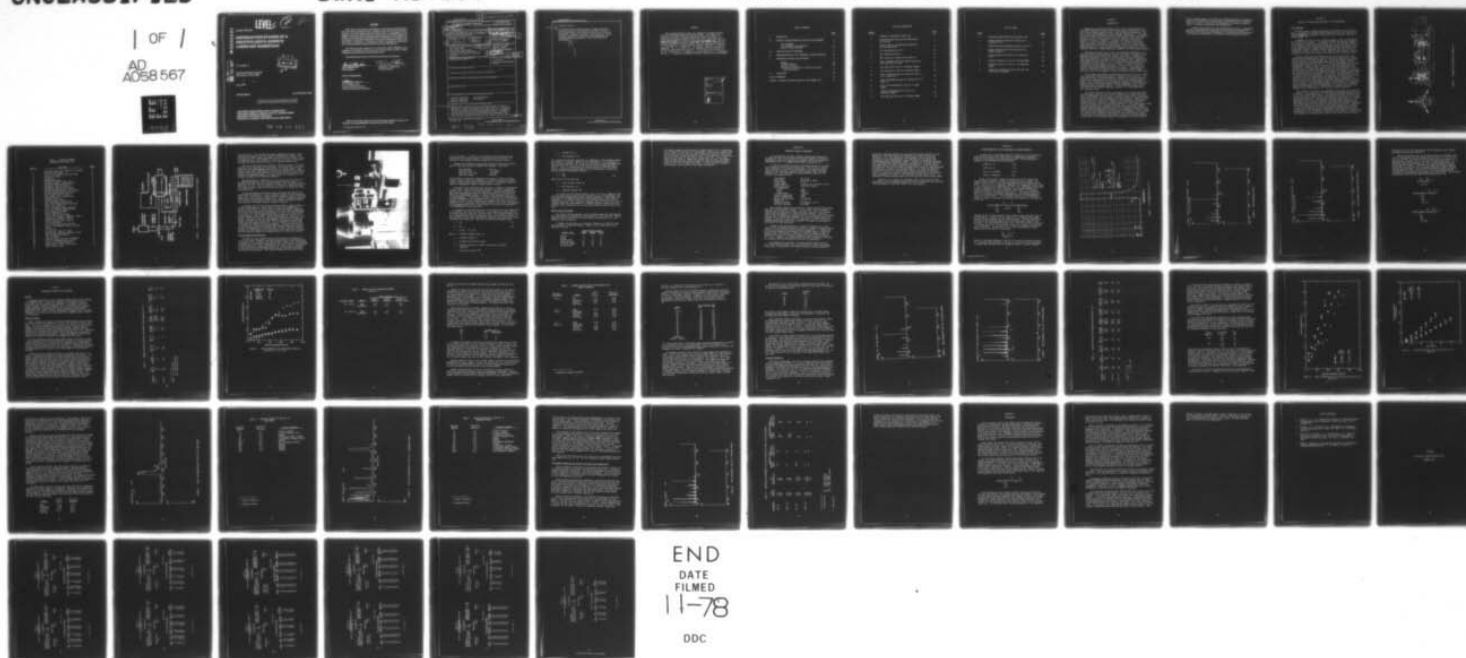
SWRI-RS-659

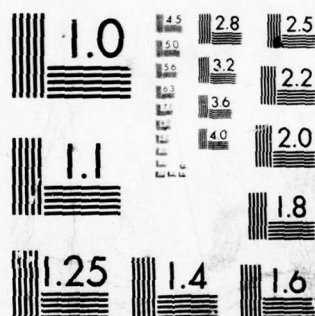
AFAPL-TR-78-46

NL

1 OF 1

AD
A058 567





MICROCOPY RESOLUTION TEST CHART
NATIONAL BUREAU OF STANDARDS-1963-A

LEVEL II

②

J

AD A058567

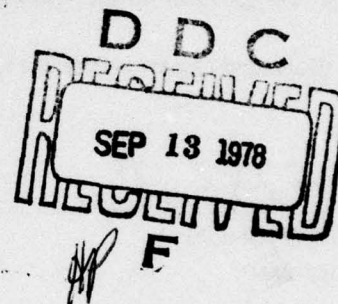
AFAPL-TR-78-46

**DEGRADATION STUDIES OF A
DI(2-ETHYLHEXYL) ADIPATE
LUBRICANT BASESTOCK**

DDC FILE COPY

J.P. Cuellar, Jr.

Southwest Research Institute
San Antonio, Texas 78284



June 1978

Interim Report

July 1977-March 1978

Approved for public release; distribution unlimited

**AIR FORCE AERO PROPULSION LABORATORY
AIR FORCE WRIGHT AERONAUTICAL LABORATORIES
AIR FORCE SYSTEMS COMMAND
WRIGHT-PATTERSON AIR FORCE BASE, OHIO 45433**

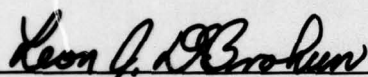
78 09 08 015

NOTICE

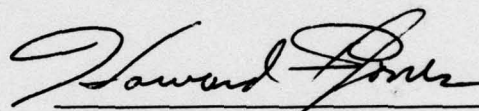
When Government drawings, specifications, or other data are used for any purpose other than in connection with a definitely related Government procurement operation, the United States Government thereby incurs no responsibility nor any obligation whatsoever; and the fact that the government may have formulated, furnished, or in any way supplied the said drawings, specifications, or other data is not to be regarded by implication or otherwise as in any manner licensing the holder or any other person or corporation, or conveying any rights or permission to manufacture, use, or sell any patented invention that may in any way be related thereto.

This report has been reviewed by the Information Office (ASD/OIP) and is releasable to the National Technical Information Service (NTIS). At NTIS, it will be available to the general public, including foreign nations.

This technical report has been reviewed and is approved for publication.

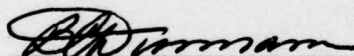


LEON J. DEBROHUN
Project Engineer



HOWARD F. JONES, Chief
Lubrication Branch

FOR THE COMMANDER



B. C. DUNNAM, Chief
Fuels and Lubrication Division
Air Force Aero Propulsion Laboratory

Copies of this report should not be returned unless required by security consideration, contractual obligations, or notice on a specific document.

Unclassified

SECURITY CLASSIFICATION OF THIS PAGE (When Data Entered)

SWRI-RS-659

REPORT DOCUMENTATION PAGE		READ INSTRUCTIONS BEFORE COMPLETING FORM
1. REPORT NUMBER AFAPL TR-78-46	2. GOVT ACCESSION NO.	3. RECIPIENT'S CATALOG NUMBER
4. TITLE (and Subtitle) DEGRADATION STUDIES OF A DI(2-ETHYLHEXYL) ADIPATE LUBRICANT BASESTOCK		5. TYPE OF REPORT & PERIOD COVERED Interim Report Jul 77 - Mar 78 PERFORMING OR REPORT NUMBER RS-659
7. AUTHOR(s) J. P. Cuellar, Jr	8. CONTRACT OR GRANT NUMBER(s) F33615-76-C-2020	
9. PERFORMING ORGANIZATION NAME AND ADDRESS Southwest Research Institute 6220 Culebra Road San Antonio, Texas 78284		10. PROGRAM ELEMENT, PROJECT, TASK AREA & WORK UNIT NUMBERS Project No. 3048 Task No. 304806 Work Unit No. 30480687
11. CONTROLLING OFFICE NAME AND ADDRESS Air Force Aero Propulsion Laboratory AFAPL/SFL Wright-Patterson Air Force Base, Ohio 45433		12. REPORT DATE June 1978 13. NUMBER OF PAGES 59
14. MONITORING AGENCY NAME & ADDRESS (if different from Controlling Office)		15. SECURITY CLASS. (of this report) Unclassified 15a. DECLASSIFICATION/DOWNGRADING SCHEDULE
16. DISTRIBUTION STATEMENT (of this Report) Approved for public release; distribution unlimited		
17. DISTRIBUTION STATEMENT (of the abstract entered in Block 20, if different from Report)		
18. SUPPLEMENTARY NOTES		
19. KEY WORDS (Continue on reverse side if necessary and identify by block number) Synthetic lubricants Lubricant analysis Lubricant degradation Test methods Lubricant deposition		
20. ABSTRACT (Continue on reverse side if necessary and identify by block number) Employing a device known as the rotating cylinder rig for the formation of controlled-thickness thin films (0.004 in.), studies are described to examine the mechanisms of degradation of an uninhibited diester lubricant basestock, di(2-ethylhexyl) adipate. Experiments were performed to investigate the thermal (inert atmosphere) and oxidative (air atmosphere) stability of the diester, and the effect		

DD FORM 1473
1 JAN 73

EDITION OF 1 NOV 65 IS OBSOLETE

Unclassified

SECURITY CLASSIFICATION OF THIS PAGE (When Data Entered)

328 200 78 09 08 015

Unclassified

SECURITY CLASSIFICATION OF THIS PAGE (When Data Entered)

20. ABSTRACT (Cont'd)

of moisture for both atmosphere types. Program objectives included elucidation of the chemical processes involved in fluid deterioration, particularly as related to the formation of deposits. Reactants and products were measured by various analytical techniques, principally gas chromatography, gas chromatography/mass spectrometry, and X-ray fluorescence spectrometry.

Unclassified

SECURITY CLASSIFICATION OF THIS PAGE (When Data Entered)

PREFACE

This interim technical report was prepared by the Mobile Energy Division of Southwest Research Institute (SwRI). The effort was sponsored by the Air Force Aero Propulsion Laboratory (AFAPL), Air Force Systems Command, Wright-Patterson AFB, Ohio, under Contract No. F33615-76-C-2020 for the period 1 July 1977 to 31 March 1978. The work herein was accomplished under Project 3048, Task 304806, Work Unit No. 30480687, Mechanism of Turbine Engine Lubricant Deposition, with Messrs. L. J. DeBrohun, H. A. Smith, and P. W. Centers, AFAPL/SFL, as Project Engineers. Mr. J. P. Cuellar, Jr. of Southwest Research Institute was technically responsible for the work. The technical contributions of Dr. G. E. Fodor, Mr. F. M. Newman, Dr. Carter Nulton, Mr. C. F. Rodriguez, and Mr. L. L. Stavinoha of Southwest Research Institute are acknowledged.

ACCESSION for	
NTIS	Wide Section <input checked="" type="checkbox"/>
DDC	Brief Section <input type="checkbox"/>
UNANNOUNCED	<input type="checkbox"/>
JUSTIFICATION	
BY	
DISTRIBUTION/AVAILABILITY CODES	
Dist.	SPECIAL
A	

TABLE OF CONTENTS

	<u>Page</u>
I. INTRODUCTION	1
II. ROTATING CYLINDER DEPOSITION TEST RIG AND PROCEDURES	3
Test Equipment	3
Test Procedures and Conditions	7
Deposit Rating Procedure	10
III. LUBRICANT ANALYSIS PROCEDURES	12
IV. CHARACTERIZATION OF DI(2-ETHYLHEXYL) ADIPATE BASESTOCK	14
V. EXPERIMENTAL RESULTS AND DISCUSSION	19
General	19
Thermal Stability	19
Oxidative Stability	26
Performance Comparison for Diester and Polyol Ester Basestocks	38
VI. CONCLUSIONS	42
LIST OF REFERENCES	45
APPENDIX - ROTATING CYLINDER DEPOSITION TEST SUMMARY DATA	46

LIST OF ILLUSTRATIONS

<u>Figure</u>		<u>Page</u>
1	Schematic of Rotating Cylinder Rig	4
2	Rotating Cylinder Rig Lubricant/Atmosphere Flow Systems	6
3	Overall View of the Rotating Cylinder Rig and Instrumentation	8
4	Gas Chromatogram of O-77-1	15
5	Mass Spectrum of Peak 2	16
6	Mass Spectrum of Primary Ester (Peak 3)	17
7	Ester Consumption Data for Thermal Stability Tests on O-77-1 at 575°F	21
8	Mass Spectrum of Test No. 49 Deposit Sample	27
9	Mass Spectrum of Test No. 49 Residue Sample	28
10	Ester Consumption Data for Oxidation Tests on O-77-1, Moist Air	31
11	Oxygen Consumption Values for Lubricant O-77-1, Moist Air	32
12	Total Ion Chromatogram of Test No. 44 Sump Sample	34
13	Total Ion Chromatogram of Test No. 44 Condensate Sample	36
14	Mass Spectrum of Test No. 44 Residue Sample	39

LIST OF TABLES

<u>Table</u>		<u>Page</u>
1	Rotating Cylinder Deposition Rig—Parts List	5
2	Thermal Stability End-of-Test Results for Lubricant O-77-1	20
3	Thermal Stability Breakdown Products for O-77-1	22
4	Thermal Stability Test and Molecular Still Sample Properties	24
5	Oxidation End-of-Test Results for Lubricant O-77-1	29
6	Oxidation Products in Test No. 44 Sump Sample	35
7	Oxidation Products in Test No. 44 Condensate Sample	37
8	Comparative Performance Data for Diester and Polyol Ester Basestocks	40

SECTION I

INTRODUCTION

Commercially synthesized organic esters serve as the basestock for formulated lubricants currently used for main engine lubrication in virtually all gas turbine powered aircraft, both military and commercial. Two ester classes are predominant in such lubricant formulations: (1) dibasic acid esters formed via esterification of dibasic fatty acids and monohydric alcohols, and (2) neopentyl polyol esters of monobasic fatty acids and polyhydric alcohols. Frequently, to enhance rheological properties, blends of various ester types are employed. In the case of the polyol esters particularly, mixtures of esterification acids of varying chain length may also be used for the same purpose. Both ester classes utilize selected additives to achieve improved performance in properties such as oxidation stability, sludge dispersancy, foaming, and load-carrying capacity.

After some 30 years of use, study, and continuing improvement, it is understandable that turbine engine aircraft lubricants in present service generally provide satisfactory and reliable performance. Upgrading of lubricant formulations, lubricant specifications, and engine designs has been responsible for achievement of this performance level. Opposing this improvement trend has been the rise in engine operating temperatures due to increased aircraft speeds or, in recent years, increased inlet air temperatures to boost engine efficiency. Thus, research to define and evaluate lubricant performance properties continues. Investigation concerns the suitability of present fluids for current or future engine designs, as well as the promise of newly introduced lubricant formulations.

Of the numerous performance requirements which must be met by a lubricant formulation, deposition tendency is perhaps the most critical. The deleterious effect of lubricant deposits formed in the aircraft engine is manifested by plugging of lubricant jets and filters; malfunctioning of pumps, seals, and bearings; and accompanying increases in maintenance costs. Deposits result from thermal and/or oxidative breakdown of the lubricant formulations and are formed, primarily, in high-temperature engine zones which receive only indirect lubricant wetting, i.e., areas subjected to thin lubricant films.

The overall objective of this investigation is to examine and define the mechanisms involved in the process of deposition by ester-base lubricants. Experimental work utilized a rotating cylinder device, subsequently described in detail, for the formation of thin (0.004 in.) lubricant films under conditions of controlled temperature and atmosphere. The program schedule calls for studies of a selected polyol ester basestock and a diester basestock, both with and without additives. This interim report deals only with research on an uninhibited diester, di(2-ethylhexyl) adipate. Degradation/deposition experiments with this basestock included studies of thermal (inert atmosphere) and oxidative (air atmosphere) stability, using both dry and moist atmospheres for each type of environment. Various chemical analyses were employed to quantitatively and, where possible, qualitatively monitor the reactants and products involved in the deterioration of the ester. The principal analytical techniques used for this purpose

were gas chromatography and combined gas chromatography/mass spectrometry. Values for the energy of activation were also derived from the oxidation tests on the ester. These data were determined from oxygen consumption rates as a function of lubricant film temperature.

A similar investigation with an uninhibited polyol ester, trimethylolpropane triheptanoate, was described in an earlier interim report.⁽¹⁾ That report also presented the findings of a literature search pertaining to the analysis and chemistry of ester-base turbine engine lubricants.

SECTION II

ROTATING CYLINDER DEPOSITION TEST RIG AND PROCEDURES

Test Equipment

The device used in conducting oxidative and thermal stability experiments is known as the rotating cylinder deposition test rig. Details of the background and development of the device were originally described in AFAPL-TR-75-37.(2)

A schematic of the test rig is shown in Figure 1, with an identifying parts list given in Table 1. To provide for firm mounting and alignment, the assembly is installed on a lathe bed, item 1. The cylinder, item 17, is of stainless steel (Type 304) construction, open at one end and closed at the opposite end by a hemispherical internal surface connected to the drive shaft, item 20. Nominal cylinder dimensions are 4-in. ID with a horizontal surface of 4-1/2 in. At its open end, the cylinder is sealed by means of a carbon-face bellows seal, item 15, and its housing, item 14.

Passing through the seal housing are the oil-in line, item 5, and three bare-wire thermocouples, item 6, which can be positioned in contact with the fluid film on the cylinder ID. To provide hermetic sealing and lateral movement, the thermocouple probes enter the cylinder section through small metal bellows, item 12. All three thermocouples are mounted on micrometer spindles, item 9, to allow for accurate positioning and referencing. Viewed from the cylinder open end, the thermocouple at 0° provides input to a West temperature controller which activates a pair of 8-in. clam-shell heaters (not shown) encircling the cylinder, seal housing, and exposed portion of the cylinder drive shaft. The thermocouple at 120° is used to measure film thickness. Initial film contact by this sensor is indicated by an abrupt temperature rise measured by a potentiometer. Continued insertion to contact with the cylinder wall is evidenced by an electrical resistance measurement between the thermocouple wire and the OD of the cylinder. The thermocouple sensor at the 240° position is used for precise indication of the film temperature. This sensor is a commercial microminiature element with a bead diameter of slightly less than 2 mils. Readout of this thermocouple is by electronic digital indicator.

The cylinder rig lubricant and atmosphere flow systems are illustrated in Figure 2. Both systems are sealed from the environment between the gas-in (air or N₂) and exhaust points. The unheated lubricant reservoir is of borosilicate glass, with provision for magnetic-bar stirring of the fluid. The lubricant-in pump is a Zenith precision gear pump driven by a variable speed motor, with a 10:1 speed reducer to permit stable operation. The lubricant-in line includes a 200-mesh screen filter and an electrically heated preheater coil just before the line enters the cylinder. Preheating of the test lubricant to match the target film temperature is necessary to avoid discontinuities of both film temperature and thickness on the cylinder wall. The lubricant-in temperature is monitored by a bare-wire thermocouple within the cylinder at the exit point of the oil-in line. The test lubricant is scavenged from a groove in the carbon seal counterface,

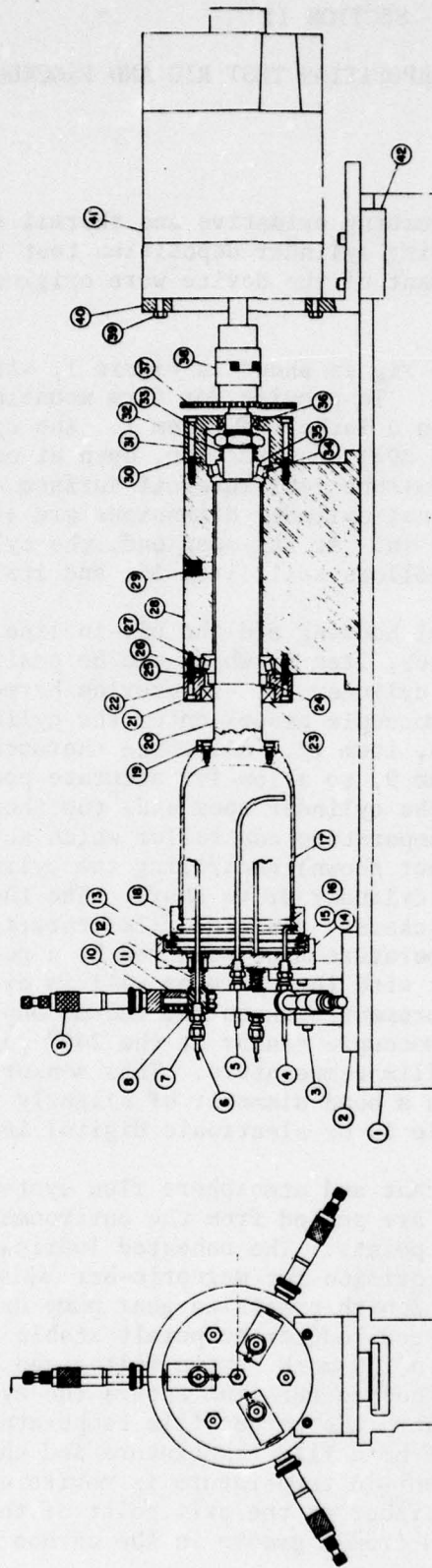


FIGURE 1. SCHEMATIC OF ROTATING CYLINDER RIG

TABLE 1. ROTATING CYLINDER
DEPOSITION RIG—PARTS LIST

Find No.	Part Name	Req'd
1	Lathe bed, Sears L9-1, Model No. 101.21400	1
2	Ring and seal bracket	1
3	1/4-20 x 3/4 hexagon socket cap screw	16
4	Scavenge oil line	1
5	Oil-in line	1
6	Thermocouple probe	3
7	Connector, Gyrolok 2 CMT-2-316	3
8	Connector adapter, SwRI A-3314-13	3
9	Micrometer, Starrett T262L-1	3
10	Micrometer ring, SwRI C-3314-15	1
11	Micrometer adapter, SwRI B-3314-16	3
12	Bellows, Metal Bellows Co. No. 60010-1	3
13	Bellows adapter, SwRI A-3314-18	3
14	Seal housing, SwRI C-3314-6	1
15	Seal, Sealol Inc. No. EJS-102573	1
16	Aluminum wire seal	1
17	Cylinder, SwRI B-3314-1	1
18	Seal counterface, SwRI B-3314-4	1
19	10-32 x 1/2 hexagon socket cap screw	4
20	Shaft, SwRI C-3314-39	1
21	10-24 x 1 hexagon socket cap screw	4
22	Front seal housing, SwRI B-3314-41	1
23	Seal, National No. 450194	1
24	Spacer, SwRI B-3314-42	1
25	O-ring, National No. 623008	2
26	Bearing cone assembly, Timken No. 13889	1
27	Bearing cup, Timken No. 13830	1
28	Bearing housing, SwRI C-3314-38	1
29	1/4-in. pipe plug	1
30	Rear seal housing, SwRI B-3314-40	1
31	10-24 x 1-3/4 hexagon socket cap screw	4
32	Spring	1
33	1-14 jam nut	1
34	Bearing cup, Timken No. 07196	1
35	Bearing cone assembly, Timken No. 07100	1
36	Seal, National No. 450567	1
37	Gear, 60-teeth	1
38	Coupling, Boston Gear No. FCR-FCBB-15	1
39	3/8-16 x 1 hexagon head cap screw	4
40	Motor bracket, SwRI D-3314-30	1
41	Boston Gear, 1/3 HP DC shunt motor	1
42	Motor bracket clamp	2

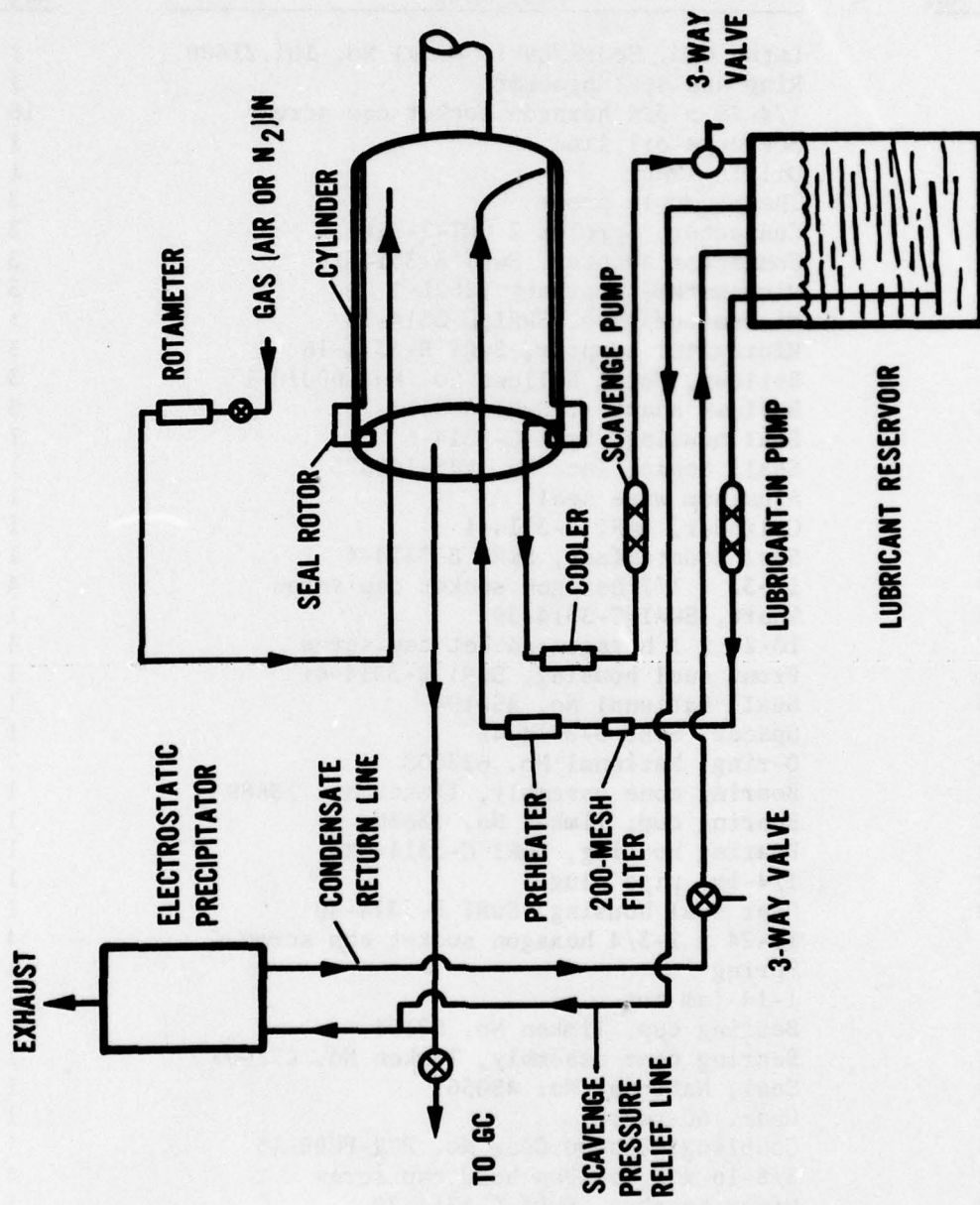


FIGURE 2. ROTATING CYLINDER RIG LUBRICANT/ATMOSPHERE FLOW SYSTEMS

item 18 (Fig. 1). The scavenge line passes immediately through a water-cooled heat exchanger (Fig. 2) to quench the degradation process. The scavenge pump, also a Zenith gear type, directs the fluid through a three-way sampling valve to the reservoir. Since over-scavenging is necessary, scavenged gas flows from the reservoir via a pressure relief line.

Gas (air or N₂) flow to the cylinder is metered through a line which exits near the closed end of the cylinder. The effluent gas line may be sampled for gas chromatographic (GC) analysis of oxygen content. Downstream of this point, the effluent line from the cylinder and the scavenge pressure relief line merge and flow to an electrostatic precipitator for recovery of condensable vapors. By gravity feed, the condensate is continuously returned to the lubricant reservoir.

The precipitator is composed of a 12-in. section of 2-in. pipe with an insulated precipitator wire centrally mounted within the pipe. In operation, the pipe section is grounded and 9000 volts of negative polarity applied to the wire. The entire device is encased by a short section of 8-in. pipe to contain debris in the unlikely event of a detonation within the precipitator.

At the precipitator operating voltage, there was some concern that, under oxidative conditions, a corona discharge capable of ozone generation might occur. Since ozone is highly reactive, oxidative attack of lubricant vapors within the precipitator might occur. However, atmosphere sampling just inside the precipitator exhaust line by means of a highly sensitive ozone detector (0.01 ppm) showed no evidence of the gas.

An overall view of the cylinder rig installation is seen in Figure 3. The gas chromatograph for oxygen analysis of the rig effluent gas is located at the far left. The cylinder, covered with blanket insulation, and the cylinder drive motor are mounted on the table near the photograph left center. The high-voltage precipitator is seen to the left and rear of the cylinder. Test lubricant pumps and the lubricant reservoir are mounted beneath the rig table. The rig instrumentation cabinet is at the center. The bench at the far right supports a strip-chart recorder and digital integrator on the lower shelf for the recording and processing output from the oxygen analysis GC. The GC instrument at the far right is used for the analysis of lubricant samples. The output from this GC is processed by a computer controlled data system subsequently described. Some of the components of this system seen in Figure 3 are the terminal teletype, the analog/digital (A/D) converter to the right of the teletype, and the acoustical coupler and telephone below the strip-chart recorder.

Test Procedures and Conditions

Cylinder rig tests reported herein were conducted in multiples of 5 hr of test time. Normally, runs were performed with two-shift operation to obtain 15 hr of continuous run time per day. During a run, verification and recording of flow rates, temperatures, and film thickness were performed at 30-min intervals. Rotational speed of the cylinder was also recorded at this time, but speed adjustments were made, as required, to maintain the desired film thickness. Test lubricant samples (10 cm³) were taken

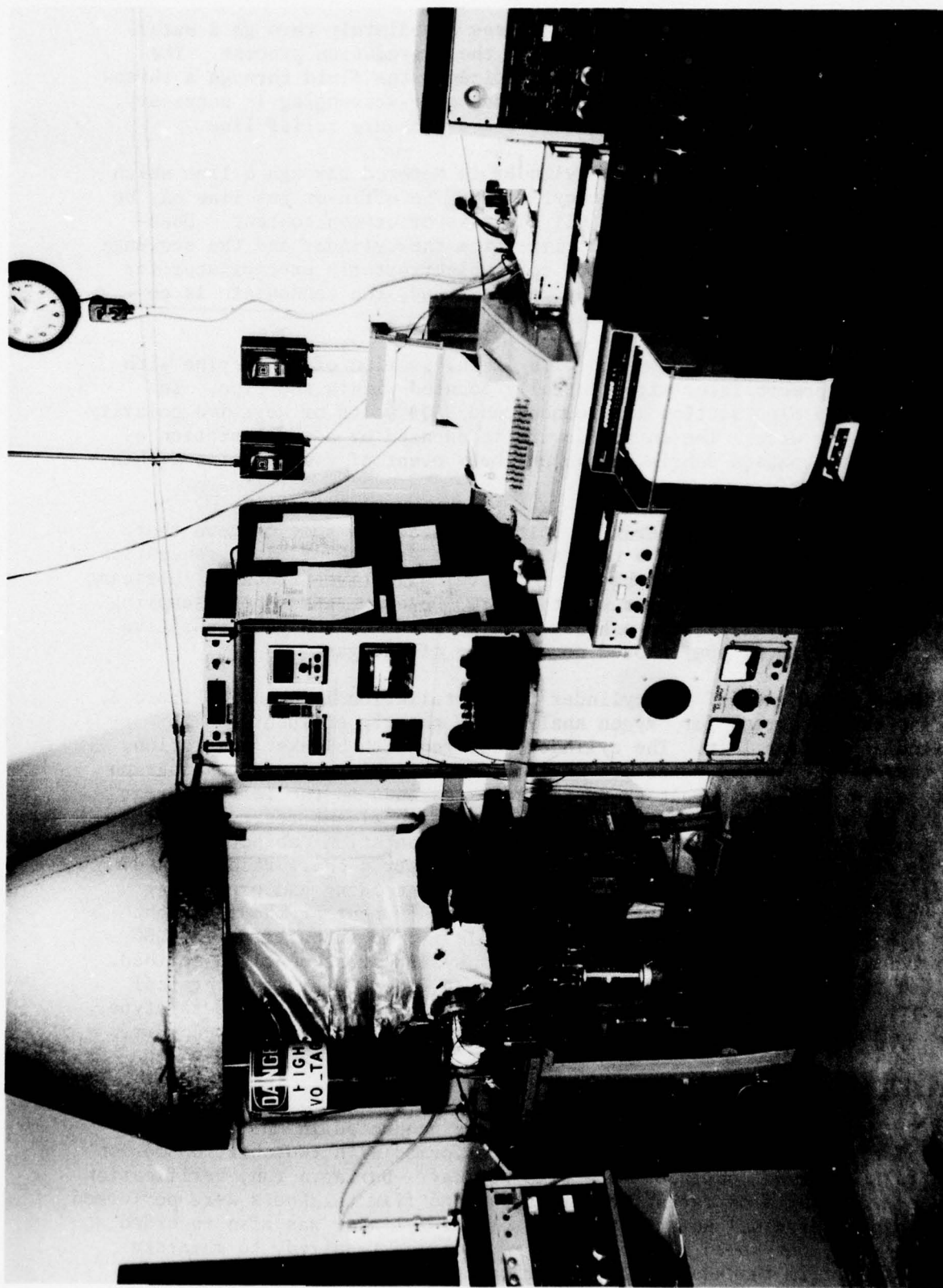


FIGURE 3. OVERALL VIEW OF THE ROTATING CYLINDER RIG AND INSTRUMENTATION

at 5-hr intervals. A sample of the condensate from the electrostatic precipitator was normally taken at the termination of each test. GC analysis of the cylinder effluent atmosphere was made each 30 min.

Certain test conditions, with values selected on the basis of prior work,⁽²⁾ were held constant throughout the program. These were:

Film thickness	0.004 in.
Lubricant flow	10 cm ³ /min
Gas (air or N ₂) flow	100 l/hr
Lubricant charge	1000 cm ³

Test duration was generally dictated by the extent of lubricant deterioration. That is, runs were terminated if excessive increases in sample viscosity and/or neutralization number occurred. No lubricant makeup for losses or intermediate samples was made during the tests.

Three major test conditions were varied as a subject of investigation in this study. These were atmosphere (oxidative or inert), atmosphere moisture (dry or moist), and film temperature. Thermal stability experiments were performed with inert gas (N₂) blanketing of the cylinder rig lubricant and atmosphere systems. Oxidative tests employed filtered air as the atmosphere. The presence or absence of moisture was investigated for both atmospheres. Dry atmosphere tests used a gas (air or N₂) of -95°F dewpoint or below. Moist atmosphere runs employed a gas with a moisture content of 10 ± 1 mg/liter. The thermal stability test series was conducted at film temperatures of 575°F; the oxidative test series was performed at film temperatures of 350° and 375°F.

In addition to the specification of test conditions of film temperature, film thickness, and total oil flow rate, calculations were made relative to average and total lubricant residence times. The average residence time was a calculated value for a "single pass" based on the average velocity of the lubricant, which in turn was based on lubricant flow rate and the cross-sectional area of the film. Thus, the following relationships apply:

$$t = l/v \quad (1)$$

$$v = Q/c \quad (2)$$

$$c = \pi/4[d^2 - (d - h)^2]$$

where t = average residence time, sec

l = cylinder length, cm

v = average film velocity, cm/sec

Q = lubricant flow rate, cm³/sec, corrected for thermal expansion

c = film cross section, cm²

d = cylinder ID, cm

h = film thickness, cm

It is noted that the above relations are simplified in that boundary effects and, possibly, rotational effects are not considered. If one considers a unit volume of lubricant, the volume will be exposed to the high-temperature cylinder surface in one cycle for the duration of the average residence time, t . If it is assumed that each fluid increment has an equal probability of undergoing the same number of cycles during test, a total residence time may be calculated as follows:

$$E = \frac{TQt}{V} \quad (3)$$

where Q and t are as above and

E = total residence time, sec

T = test duration, sec

V = lubricant charge, cm^3

To account for fluid losses during a test, Eq. (3) was summed for each 5-hr test period using a mean volume indicated by oil loss measurement, and correcting for intermediate lubricant sample withdrawals. Under these circumstances, it is observed that the total residence time per 5-hr period increases with test time. Similarly, unusually high oil losses (e.g., due to improper carbon-seal performance of a temporary nature) increase the total residence time, especially if the losses occur during the early hours of the test.

Deposit Rating Procedure

The deposit rating procedure used to describe numerically the deposits occurring within the cylinder was essentially that used in the 48-hr bearing deposition test(3) except that only one surface was inspected, viz., the surface of the cylinder ID.

A demerit rating number was selected to identify the different types and thicknesses of deposits present. Demerit values range from 0 to 20, defined as follows:

<u>Deposit Type</u>	<u>Demerit Rating Number</u>		
	<u>Light</u>	<u>Medium</u>	<u>Heavy</u>
Varnish	1	3	5
Sludge	6	7	8
Smooth carbon	9	10	11
Crinkled carbon	12	13	14
Blistered carbon	15	16	17
Flaked carbon	18	19	20

This demerit number was multiplied by a number from 0 to 10, corresponding to the percent of the area, 0 to 100 percent, covered by that deposit type. In the event that more than one type of deposit was present on the rated area, the deposit rating was then the total of the individual rating values necessary to account for 100 percent of the rated area. In any event, double ratings, such as sludge over varnish, were not used. The deposit rated was that which was visible without the removal of another deposit, except in the case of sludge over carbon. In such instances, the more severe deposit type was used in the rating calculations.

SECTION III

LUBRICANT ANALYSIS PROCEDURES

All intermediate and final lubricant samples taken during the cylinder rig tests were routinely analyzed for kinematic viscosity by ASTM Method D 445 and for neutralization number (total acid number) by ASTM Method D 664. All samples were likewise analyzed by GC.

GC was the principal tool used in following changes in the major ester component of the lubricant basestock, as well as other significant constituents in the new or used samples. The analysis was performed with an instrument equipped with a hydrogen flame ionization detector (FID). The conditions and column materials used with the procedure are summarized here:

Liquid phase	OV-17, 2%
Solid phase	Gas Chrom Q, 60/80
Column length	17 ft
Column tubing	0.125-in. OD x 0.093-in. ID S.S.
Column efficiency	1025 theor. plates
Oven temperature	
Initial	180°C
Final	300°C
Program rate	8°C/min
Injector temperature	300°C
Detector temperature	320°C
Carrier gas (He) flow	25 cm ³ /min
Sample size	0.2 µl
Internal standard	n-tridecane, 10 wt %
Injection procedure	On-column

The GC output signal was processed by a Hewlett-Packard 3354A laboratory data system available at SwRI. In this system, the A/D converter digitizes the GC signal and transmits the data via a cable loop (serving several SwRI laboratories) to a general purpose computer. Analytical results from the computer and report print-outs are received by the terminal teletype over a direct-wired telephone line, with associated acoustical couplers at each end of the line. The availability of this system to the program significantly benefitted the effort with regard to the accuracy and speed of GC data processing.

Because of the unavailability of suitable standards and, in some cases, of full knowledge of chemical structure, a common GC response factor relative to n-C₁₃ was used for all lubricant components. It should also be noted that component concentrations for degraded samples, reported as weight percent, are subject to some error since no attempt was made to achieve total recovery of gaseous degradation products such as moisture, CO, or CO₂. However, it is believed that the error introduced by the lack of a material balance determination would not be appreciable.

The adipate ester basestock, selected degraded samples thereof, and selected deposit samples were also analyzed by various other methods in an effort to characterize the chemical structure of these materials.

Analytical techniques utilized for this purpose included infrared spectrophotometry, X-ray fluorescence spectrometry, short-path distillation (molecular still), gel permeation chromatography, reversed-phase high performance liquid chromatography, mass spectrometry, and combined gas chromatography/mass spectrometry (GC/MS). Analyses by GC/MS were performed with a Finnigan Model 3300F instrument interfaced with a computer for both instrument control and data acquisition and analysis. The GC procedures and conditions used with the GC/MS instrument were similar to those previously described for GC analysis of lubricant samples. The GC/MS instrument may be operated by use of an electron impact ionization source (70 electron volts) or a chemical ionization source (methane reagent gas), each equipped with a quadrupole mass filter. The GC/MS facility has access to the Cyphernetics spectra library known as the mass spectral search system (MSSS).

Selection of the analytical procedures used in this study was based principally on prior knowledge of the field and the findings of the literature search presented in a previous report⁽¹⁾ on this program.

CHARACTERIZATION OF DI(2-ETHYLHEXYL) ADIPATE BASESTOCK

100°F Vis, cs	8.19
210°F Vis, cs	2.37
Neut. No., mg KOH/g	0.03
Gravity, °API/60°F	21.0

$$\begin{array}{c} \text{CH}_3(\text{CH}_2)_3\text{CHCH}_2-\text{O}-\overset{\text{O}}{\parallel}\text{C}-(\text{CH}_2)_4-\overset{\text{O}}{\parallel}\text{C}-\text{O}-\text{CH}_2\text{CH}(\text{CH}_2)_3\text{CH}_3 \\ | \qquad \qquad \qquad \text{MW } 370 \qquad \qquad \qquad | \\ \text{CH}_2 \qquad \qquad \qquad \qquad \qquad \qquad \qquad \text{CH}_2 \\ | \qquad \qquad \qquad \qquad \qquad \qquad \qquad | \\ \text{CH}_3 \qquad \qquad \qquad \qquad \qquad \qquad \qquad \text{CH}_3 \end{array}$$
$$\begin{array}{c} \text{O} \quad \quad \text{O} \\ ||| \quad \quad || \\ \text{C}(\text{CH}_2)_4\text{C}-\text{OH} \end{array} \quad 7 +$$

14

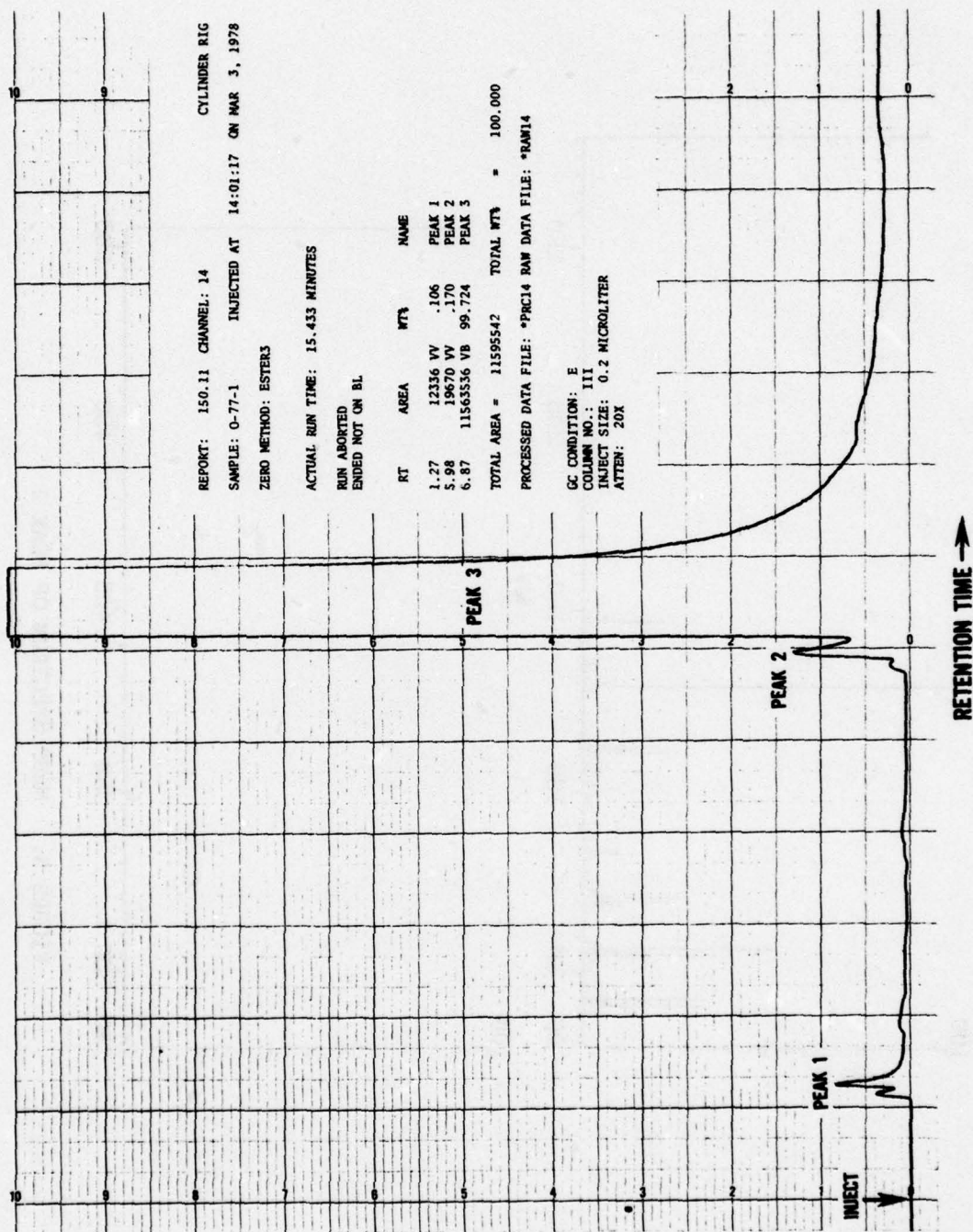


FIGURE 4. GAS CHROMATOGRAM OF 0-77-1

817K04 Y-1000 DI(2-ETHYLHEXYL)ADIPATE GC/EI
159 -154 RT=5.73 MIN

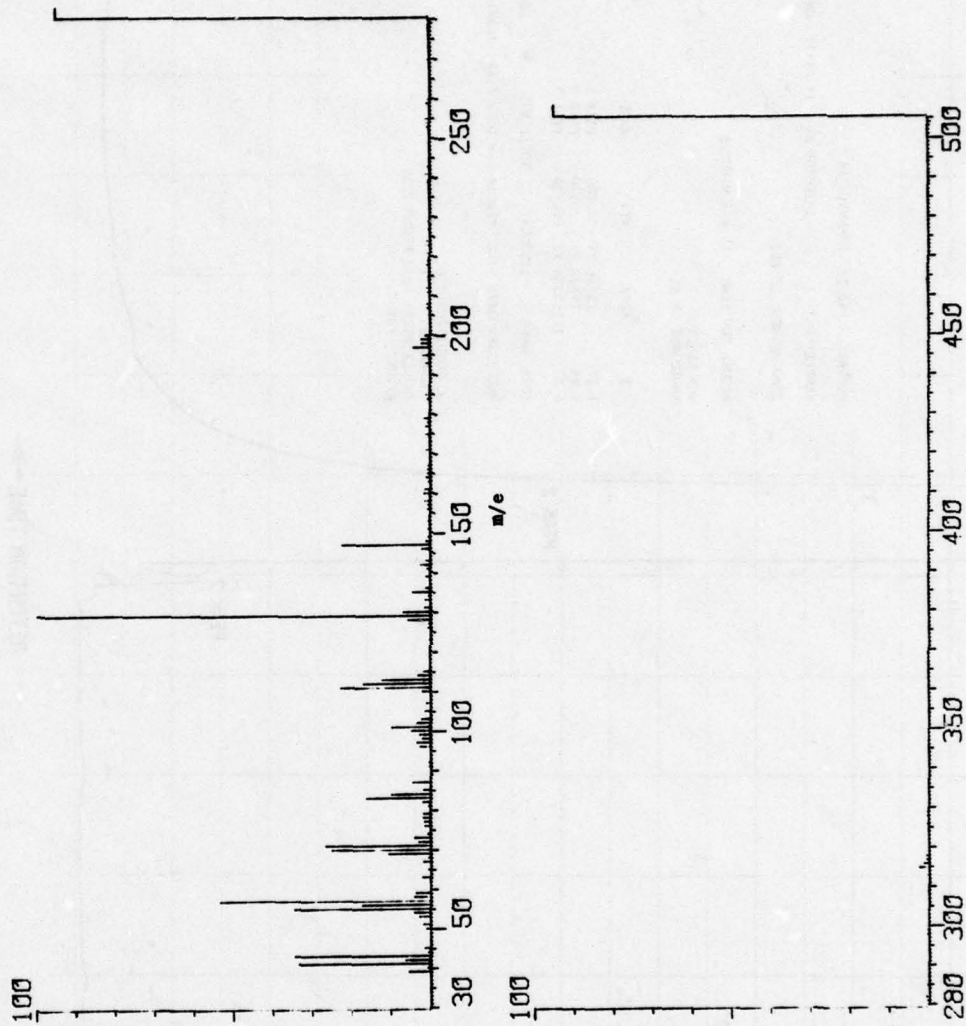


FIGURE 5. MASS SPECTRUM OF PEAK 2

817K04 Y-1000 DI(2-ETHYLHEXYL)ADIPATE GC/EI
 # 165 -169 RT=5.95 MIN

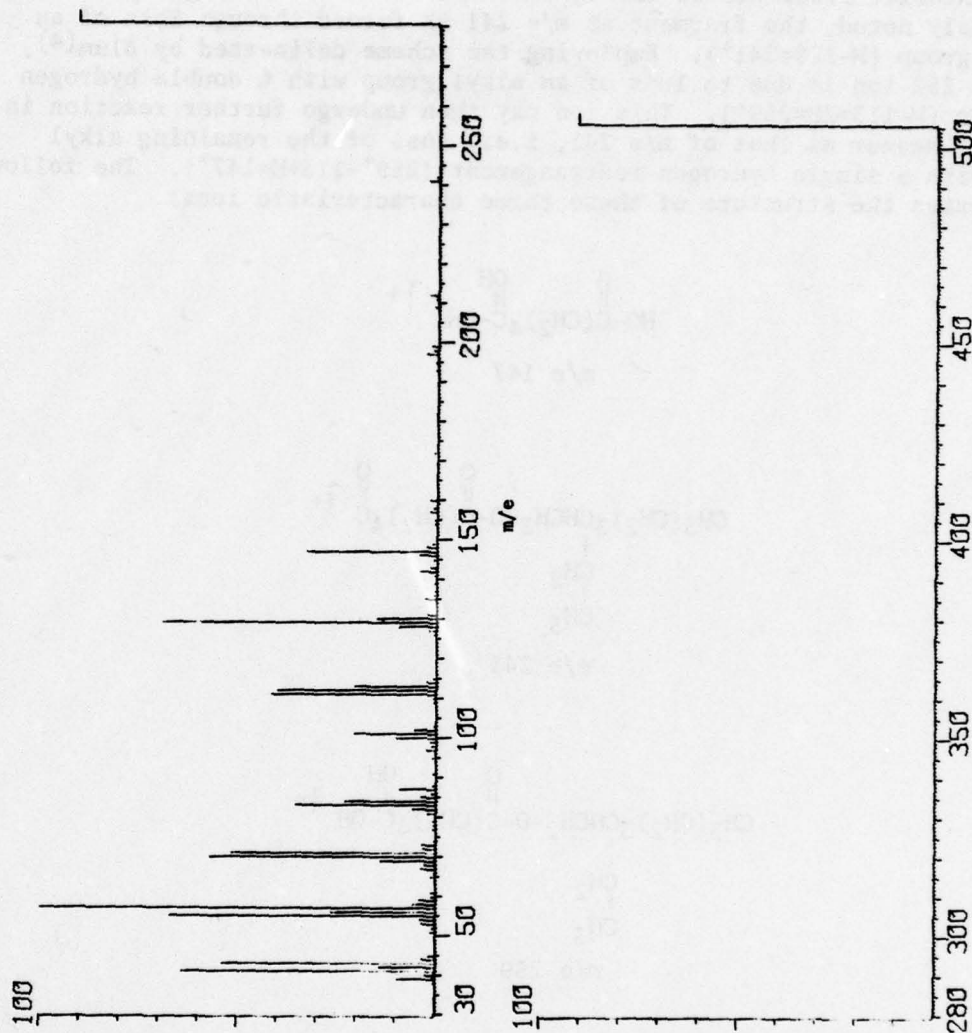
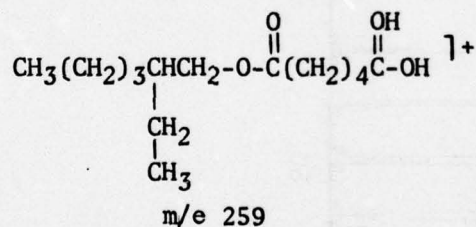
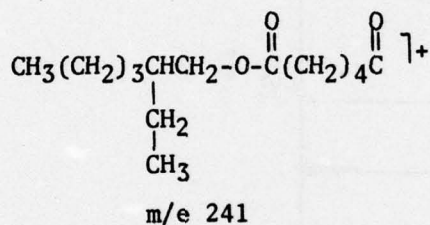
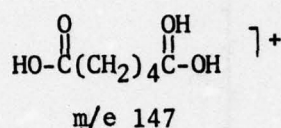


FIGURE 6. MASS SPECTRUM OF PRIMARY ESTER (PEAK 3)

structure in one of the alcohol groups, which difference is not readily discernible from the mass spectrum.

Other characteristic ions in the mass spectrum of the primary ester (Fig. 6) which should be noted include those at m/e 55, 57, 70, 71, 112, 147, 241, and 259. The first five ions of this series are believed to be representative fragments of the alkyl chain of the alcohol group. As previously noted, the fragment at m/e 241 is formed through loss of an alkoxy group ($M-129=241^+$). Employing the scheme delineated by Blum⁽⁴⁾, the m/e 259 ion is due to loss of an alkyl group with a double hydrogen transfer ($M-113+2H=259^+$). This ion may then undergo further reaction in the same manner as that of m/e 241, i.e., loss of the remaining alkyl group with a single hydrogen rearrangement ($259^+-113+H=147^+$). The following illustrates the structure of these three characteristic ions:



SECTION V

EXPERIMENTAL RESULTS AND DISCUSSION

General

Individual data sheets for all rotating cylinder rig tests are included in the Appendix hereto. These data summaries are arranged in order of test number and list pertinent test conditions, the cylinder rig deposit rating, and basic lubricant performance data. In oxidative (air) tests, oxygen consumption values are expressed in liters at operating temperature and pressure (OPT), corresponding to ambient atmospheric pressure and temperature (75° to 80°F). Data for the amount of unreacted ester remaining, determined by GC, refer only to the primary ester component (peak 3) present in the basestock.

Thermal Stability

Table 2 presents the results of duplicate determinations with the diester basestock at 575°F film temperature, for both a dry and moist nitrogen atmosphere. For the dry nitrogen runs, the end-of-test sample showed only slight changes in fluid viscosity and neutralization number. However, deposit formation was relatively severe as evidenced by light smooth carbon (LSC) deposits, and 5 percent medium flaked carbon (MFC) for Test No. 49. Measurable consumption of the diester occurred for the dry atmosphere as indicated by values for the unreacted ester amount. Appreciable amounts of high-boiling material not eluted by GC analysis (GC residue) were also noted.

With the exception of neutralization number change, the results of Table 2 show a beneficial effect for the presence of moisture in the deterioration of the adipate diester. The extent of ester consumption was significantly reduced as shown by Table 2 and the plot of Figure 7. Moisture also resulted in a much less severe deposit type. The light varnish observed for the moist nitrogen atmosphere was a light, straw-colored deposit of no perceptible thickness.

Analyses by GC and GC/MS were carried out on samples from Tests No. 49 and 51 to establish the products of thermal degradation of the diester. The samples included both the end-of-test sump fluid and the end-of-test condensate sample taken from the return line of the electrostatic precipitator. Aside from the components identified as GC residue, which constituted the major breakdown products, the sump and condensate samples contained only a few low-boiling constituents formed, apparently, from the alcohol group of the diester. Due to volatility effects, the components were concentrated in the condensate samples and were identified as 2-ethyl-1-hexene, 2-ethyl-1-hexanol, and 2-ethyl-1-hexanoic acid. The distribution of these compounds, determined for the sump and condensate samples, is shown in Table 3. The higher free alcohol content for Test No. 49 could explain, in part, the reduced sample (sump) viscosity noted for this run. Similarly, the higher free acid content observed for the moist nitrogen determination could

TABLE 2. THERMAL STABILITY END-OF-TEST RESULTS FOR LUBRICANT O-77-1

Atmosphere	Film Temp, °F	Test Duration, hr	Total Res Time, sec	100°F Vis Incr, %	NN Change, mg KOH/g	Deposit Coverage*	Unreacted Ester, wt %	GC Residue, wt %	Test No.
Dry N ₂	575	75	926	-1	0.62	95% LSC	83.0	13.9	49
	575	75	904	-2	1.54	5% MFC 100% LSC	88.0	7.8	50
Moist N ₂	575	75	902	2	5.33	100% LV	95.3	3.4	51
	575	75	897	2	5.27	100% LV	95.2	3.8	52

*Legend: LV - light varnish
LSC - light smooth carbon
MSC - medium smooth carbon

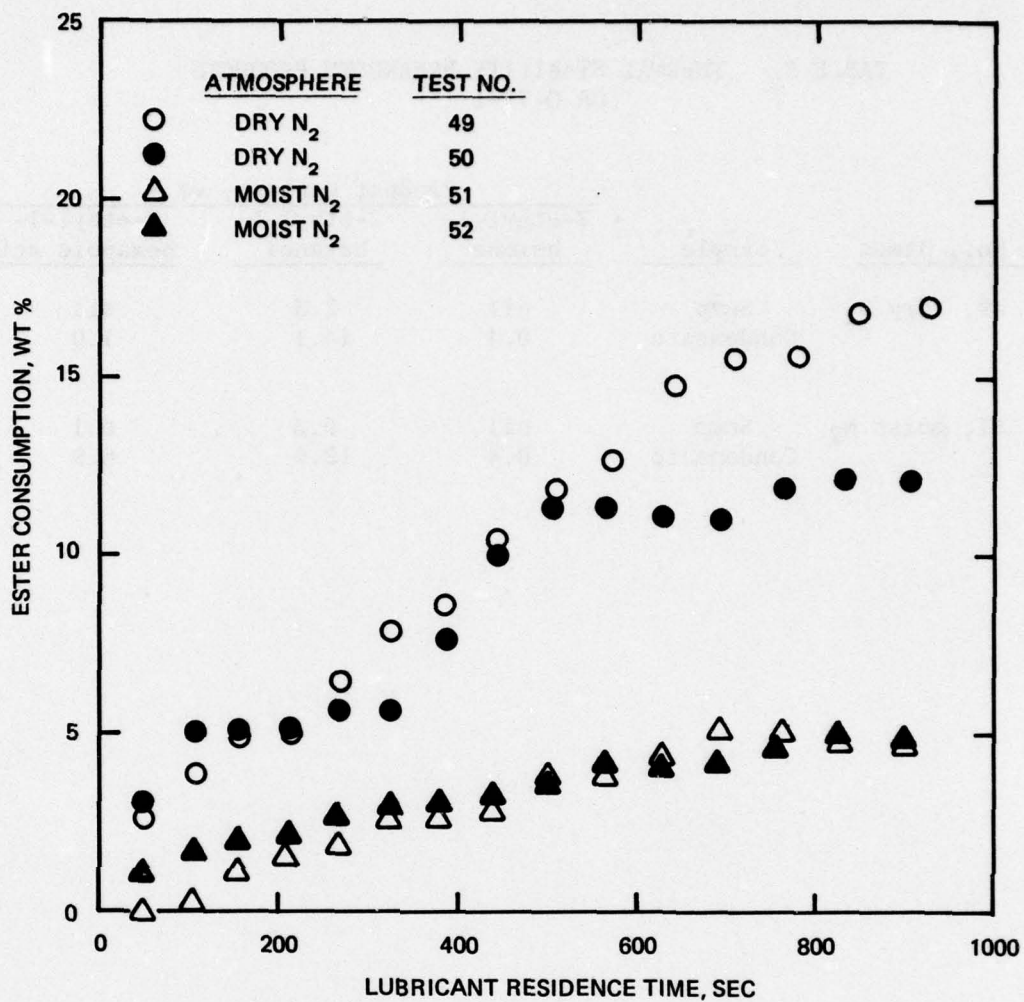


FIGURE 7. ESTER CONSUMPTION DATA FOR THERMAL STABILITY TESTS ON O-77-1 AT 575°F

TABLE 3. THERMAL STABILITY BREAKDOWN PRODUCTS
FOR O-77-1

Test No., Atmos	Sample	Product Content, wt %		
		2-ethyl-1-hexene	2-ethyl-1-hexanol	2-ethyl-1-hexanoic acid
49, dry N ₂	Sump	nil	2.3	nil
	Condensate	0.4	14.1	1.0
51, moist N ₂	Sump	nil	0.3	0.1
	Condensate	0.4	12.0	6.9

partially account for the higher neutralization number obtained for Test No. 51.

Studies by others have indicated that one major product of the thermal degradation of dibasic acid esters is the half-acid ester (mono-ester). For the conditions investigated here, there were no detectable amounts of the adipate mono-ester formed. It is conceivable that this compound, if generated, was an intermediate in the formation of the GC residue material. (A GC "standard" for the mono-ester, 2-ethylhexyl hydrogen adipate, was generated by heating an equimolal mixture of the diester and adipic acid for 48 hr at 392°F under a nitrogen blanket. The mono-ester yield in the fluid was 6 wt percent.)

Since the high-boiling ($>1000^{\circ}\text{F}$) components described as GC residue represented the major portion of degradation products formed in the thermal stability test series, further work with the end-of-test sump samples from Tests No. 49 and 51 was conducted by separations using a molecular still apparatus. Sample charges were separated under conditions of 230°F and 5×10^{-4} torr. Three sample fractions for each test resulted from the distillation: a clear, volatile fluid recovered from the dry ice trap; a light, straw-colored distillate; and a brown, viscous residue. On a percentage basis distillation residue amounts were less than, but directionally equivalent to, GC residue values obtained for the samples, as seen by the following weights:

Test No.	Residue, wt %	
	GC	Mole Still
49	13.9	2.2
51	3.4	0.2

A comparison of sample viscosity and neutralization number data for end-of-test sump, condensate, and distillation fractions is given in Table 4 for the unused basestock and Tests No. 49 and 51. These results indicate significant differences for the condensate and residue samples with the moist nitrogen condition. Except for the volatiles recovered from the still cold trap, the dry nitrogen test did not show any appreciable variation in viscosity or acidity among the various samples. The most outstanding feature of the data is the very high viscosity and neutralization number of the Test No. 51 residue sample—the test in which cylinder rig deposits were negligible.

Infrared spectra of the two test residue samples revealed no distinguishing absorbances for either sample. In fact, the spectra were very similar to the IR trace of the unused basestock except for weak absorbances characteristic of acid and alcohol hydroxyl groups in the residue samples.

Further characterization of the two distillation residue samples was performed using high performance liquid chromatography procedures. Analysis by gel permeation chromatography identified components of "equivalent molecular weight" of 420 in the Test No. 49 residue, and 610 in the residue from

TABLE 4. THERMAL STABILITY TEST AND MOLECULAR STILL
SAMPLE PROPERTIES

<u>Test No., Atmosphere</u>	<u>Sample</u>	<u>100°F Vis, cs</u>	<u>Neut. No., mg KOH/g</u>
0-77-1	Neat	8.19	0.03
	Distillate	8.21	0.04
	Residue	14.50	0.89
	Cold trap	*	*
49, dry N ₂	Sump	8.13	0.65
	Condensate	*	0.83
	Distillate	8.18	0.65
	Residue	9.85	2.76
	Cold trap	4.91	4.24
51, moist N ₂	Sump	8.38	5.36
	Condensate	*	12.62
	Distillate	8.49	6.22
	Residue	46.95	13.14
	Cold trap	4.09	2.92

* Insufficient sample available.

Test No. 51. Relative to the viscosity of the Test No. 51 residue, a molecular weight of 610 is unexpectedly low.

Previous studies⁽¹⁾ with a trimethylolpropane triheptanoate basestock showed a pronounced relationship between deposit formation and the presence of metals. Accordingly, analysis of samples for metal content from Tests No. 49 and 51 was also performed. Employing X-ray fluorescence (XRF) spectroscopy, significant amounts of iron and chromium were found in intermediate and final test samples from the dry nitrogen run (Test No. 49):

<u>Sample</u>	<u>Metal Content, ppm</u>	
	<u>Fe</u>	<u>Cr</u>
0-10 hr	nil	nil
15	30	nil
20	60	nil
25	85	nil
30	100	nil
35	140	nil
40	190	nil
45	250	nil
50	270	nil
55	330	40
60	350	50
65	310	50
70	320	60
75	340	65
Condensate	nil	nil
Distill. residue	1550	225

On a total weight basis, the residue sample contained approximately 10 percent of the amount of iron and chromium present in the 75-hr (sump) sample. Analysis by XRF of the corresponding fluid samples from Test No. 51 (moist N₂) indicated nil values (<6 ppm) for all samples.

Ferrographic analysis of the end-of-test sump samples was conducted by AFAPL. For the dry nitrogen test (carbon cylinder deposits), the ferrograph slide showed a large amount of metal fatigue chunks and severe wear and cutting wear particles, all of which appeared to be magnetic. The surface of most particles was metallic in appearance. Some carbon particles were also evident. Analysis of the moist nitrogen test sample (very light varnish cylinder deposits) indicated a large amount of fatigue chunks and a moderate amount of severe wear and cutting wear particles, all of which appeared to be magnetic. There was also a large amount of particles of a carbon appearance. The surface of the magnetic particles varied from metallic to complete coverage with a carbonaceous deposit. Between these extremes, particles were observed with varnish coatings and various stages of carbon-type deposits.

XRF analysis of the carbon deposit recovered from the cylinder rig for Test No. 49 indicated a total metal content of just over 10 wt percent, as seen by the following results:

<u>Metal</u>	<u>Content, wt %</u>
Fe	6.7
Mg	1.9
Al	0.9
Cr	0.5
Mn	<u>0.5</u>
	10.5

An IR trace of the deposit sample was characterized by minimal carbon-hydrogen bond absorbance; a broad band corresponding to associated -OH in acids; and weak carbonyl response.

After repeated washings with heptane, a portion of the deposit sample was examined by mass spectroscopy using solid probe insertion. The resultant mass spectrum is shown in Figure 8. The indicated fragment ions are typical of the adipate diester. As previously noted, high ion abundances at m/e 55, 57, 70, 71, and 112, describe the alcohol group. The base peak at m/e 129 and the m/e 147 ion are characteristic of the diester acyl group, whereas m/e 241 and 259 fragments represent ions resulting from loss of a single alcohol group.

In an effort to relate deposit formation with the high-boiling products of pyrolysis, a mass spectrum of the distillation residue from Test No. 49 was obtained. Since the major portion of this material would not elute by GC, the sample was admitted to the spectrometer by solid probe. Figure 9 illustrates the mass spectrum of the sample. Relative to the deposit sample, the residue spectrum shows a multiplicity of fragment ions. Nevertheless, the characteristic ions at m/e 55, 57, 70, 71, 112, 129, 241, and 259 are in evidence. It is also observed that the spectrum shows low abundance ions as high as m/e 370 (the diester molecular weight), 371, and 372. (The notation in Fig. 9 indicates a 5X signal amplification for m/e >290.)

Oxidative Stability

Cylinder rig experiments with O-77-1 using an oxidative (air) environment are summarized in Table 5. Initially, duplicate runs were conducted at 350°F film temperature employing both dry and moist air. Due to poor agreement of most data for the former condition, a third determination was performed. The third test, Test No. 48, indicated reasonable agreement with Test No. 46; however, Test No. 47 with dry air was more in line with results for the moist air atmosphere. Thus it is difficult to ascribe with certainty any effect for the presence of moisture on the deterioration of the diester as indicated by viscosity, neutralization number, oxygen consumption, etc.

228K03 #49 HEPTANE WASHED SP/EI
90

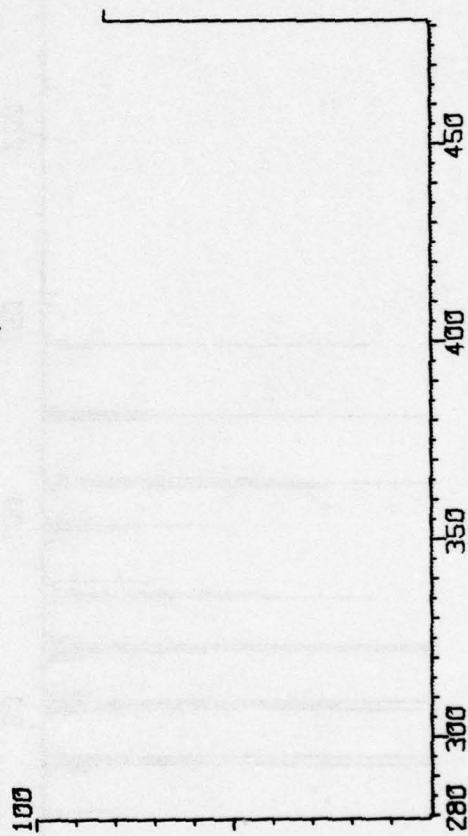
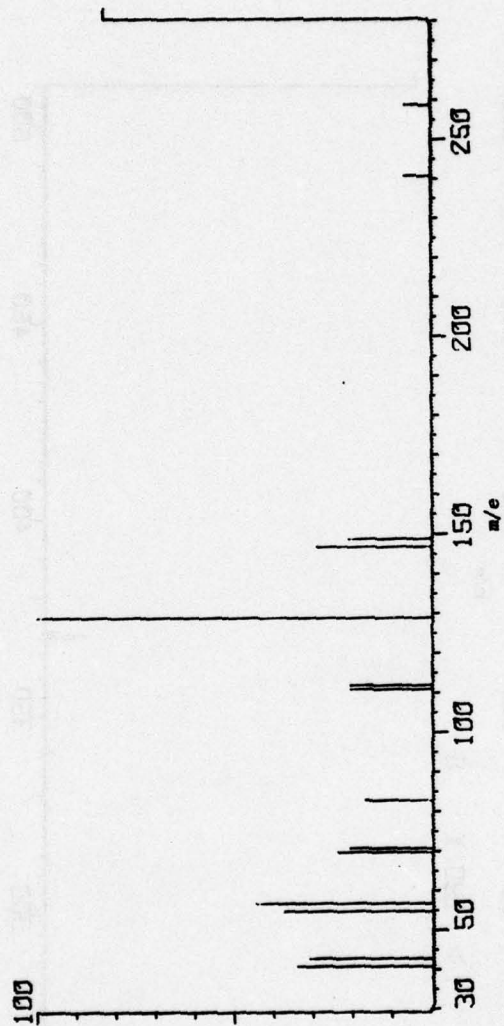


FIGURE 8. MASS SPECTRUM OF TEST NO. 49 DEPOSIT SAMPLE

413K01 TEST 49 75HRS RESIDUE (ROTA VAPOR) SP/EI
45

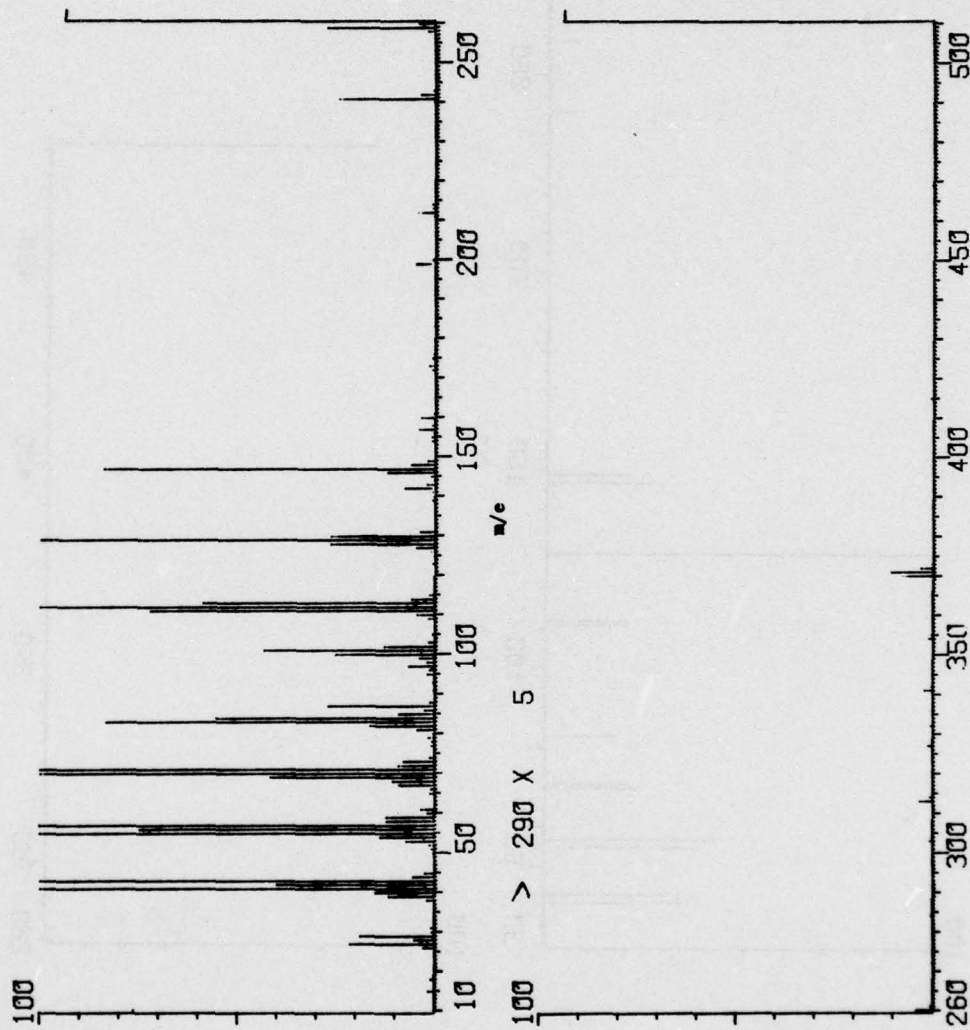


FIGURE 9. MASS SPECTRUM OF TEST NO. 49 RESIDUE SAMPLE

TABLE 5. OXIDATION END-OF-TEST RESULTS FOR LUBRICANT O-77-1

Atmosphere	Film Temp, °F	Test Duration, hr	Total Res Time, sec	100°F Vis Incr, %	NN Change, mg KOH/g	Deposit Coverage*	O ₂ Consump, % at OPT	Unreacted Ester, wt %	GC Residue, wt %	Test No.
Dry Air	350	50	622	64	23.48	100% CL	37.9	50.7	32.4	46
	350	50	670	31	13.52	100% CL	18.6	64.3	26.0	47
	350	50	674	55	22.04	100% CL	30.4	53.0	33.5	48
Moist Air	350	50	697	34	13.52	100% LV	21.6	66.3	23.3	44
	350	50	614	34	15.40	100% LV	23.4	64.8	21.7	45
Moist Air	375	35	459	39	14.09	100% LV	25.1	65.1	19.2	53
	375	35	429	40	13.35	100% LV	28.0	65.7	21.8	54

*Legend: CL - clean

LV - light varnish

A consistent effect for moisture was apparent in deposit coverage at 350°F. The dry air atmosphere produced no deposits even though virtually 50 percent of the diester was consumed, and end-of-test viscosity and neutralization number values were relatively high. Similar degradation levels were evident in the moist air tests and, in this case, light varnish (LV) deposits were noted. The material formed, however, was a very light, straw-colored deposit which indicated essentially no thickness upon scraping with a sharp instrument. In other words, the distinction between clean and light varnish deposit, though consistent in the tests, was not substantial.

The results of Table 5 for the moist air atmosphere and 375°F film temperature show that this condition produced a degradation level comparable to that for 350°F in approximately two-thirds of the exposure time. Figure 10 compares the ester consumption rates, determined by GC, for both temperatures. The plots indicate essentially a linear loss of the adipate ester throughout the tests.

The 375°F tests were performed primarily to obtain consumed oxygen rate data which would permit calculation of the energy of activation for the adipate diester using moist air. Figure 11 illustrates the data recorded for oxygen consumption. At both temperatures, the consumption rate showed a brief induction period, followed by a higher, linear consumption rate. Neglecting the induction period, the following rate values were derived by an orthogonal regression of available data:

Film Temp, °F	O ₂ Consump, ℓ/hr	Test No.
350	0.48	44
	0.59	45
375	0.91	53
	0.93	54

Using the average lubricant residence time per cycle, and assuming an exposure of 600 cm³ (10 cm³/min for 1 hr), the mean of the above oxygen consumption rates was converted to moles O₂/mole ester/sec for calculation of the energy of activation by the Arrhenius equation. A value of 16.5 K cal/mole was obtained. This compares with a value of 9.9 K cal/mole previously(1) obtained for a polyol ester basestock, trimethylolpropane triheptanoate. The higher result for the diester was unexpected. However, the energy of activation is not necessarily a criterion of the oxidative stability of the basestock and, as previously(1) noted, the data obtained for oxygen consumption are probably affected by a "rig dependence."

The products of oxidative deterioration of O-77-1 were numerous, as evidenced by GC analysis. Compounds in the boiling point range both above

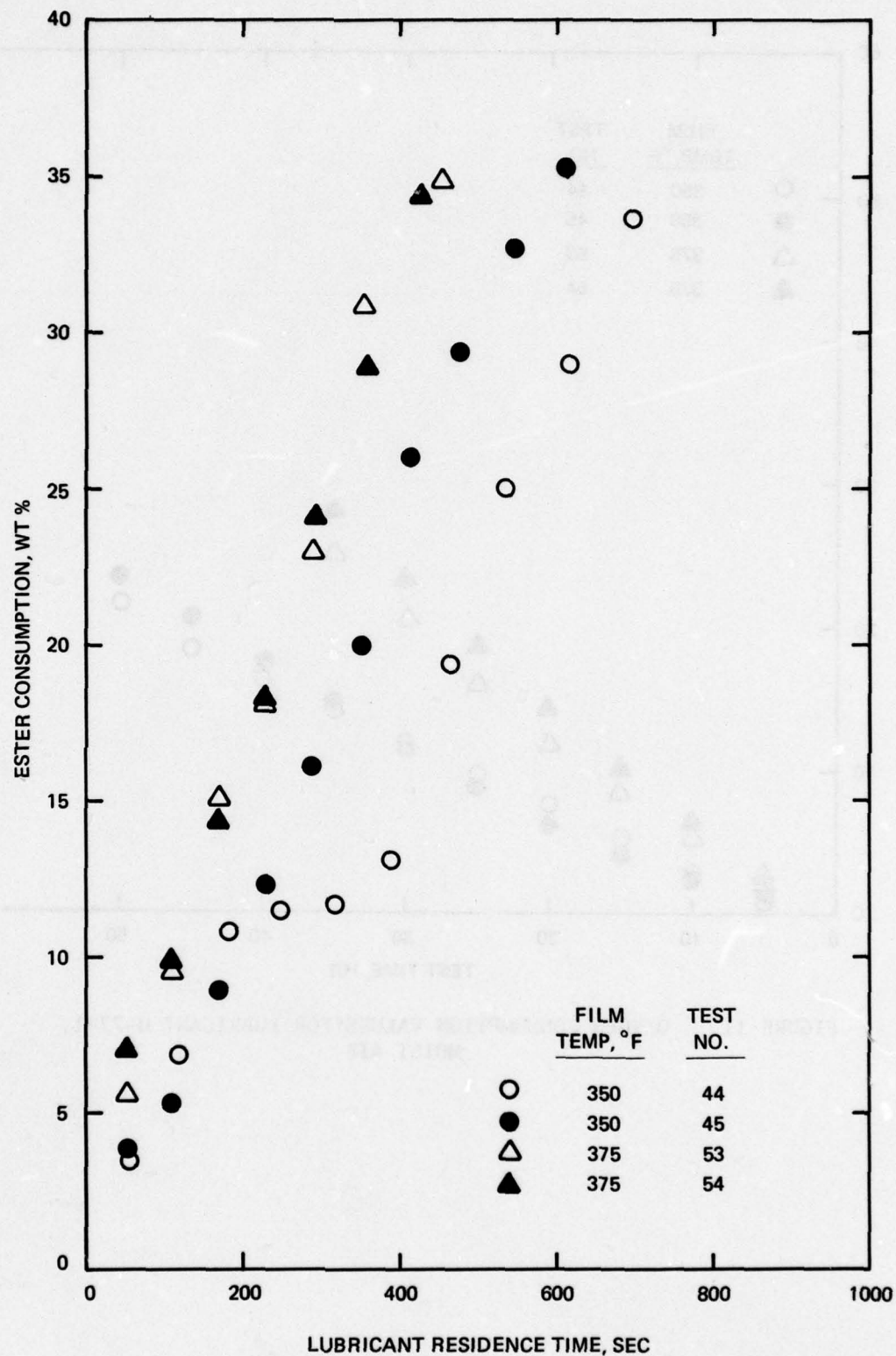


FIGURE 10. ESTER CONSUMPTION DATA FOR OXIDATION TESTS ON O-77-1, MOIST AIR

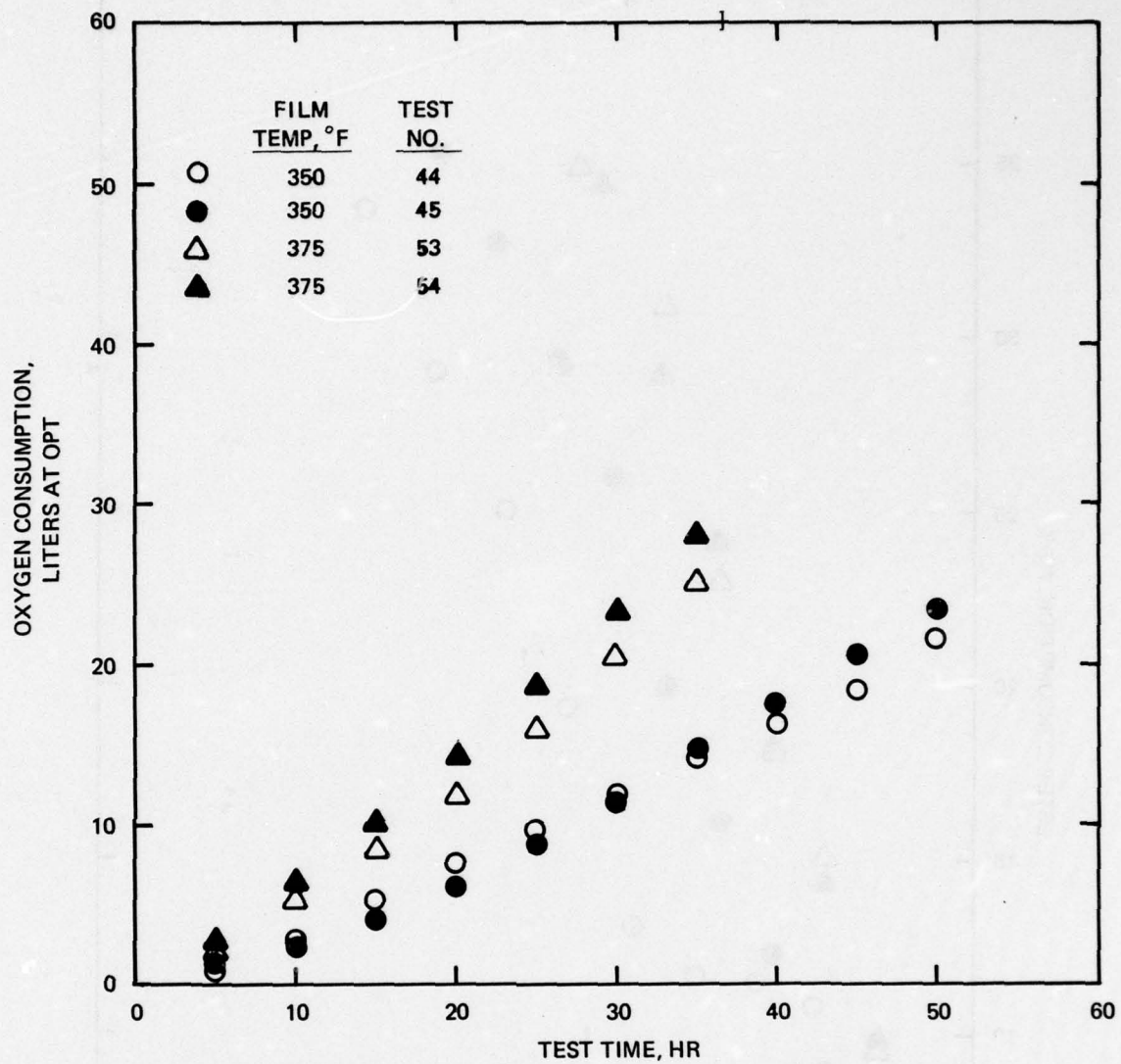


FIGURE 11. OXYGEN CONSUMPTION VALUES FOR LUBRICANT O-77-1, MOIST AIR

and below the original diester were apparent. With regard to the type and distribution of products, there was no distinguishing feature among the seven tests listed in Table 5, other than the somewhat greater degree of degradation for Tests No. 46 and 48. Accordingly, efforts concentrated on the identification of products for a single, "typical" test. Test No. 44, using moist air and 350°F film temperature, was selected for this purpose, and GC and GC/MS were the principal analytical procedures utilized.

Figure 12 presents the total ion chromatogram (TIC) generated by GC/MS for the end-of-test sump sample from Test No. 44. From the mass spectra of the major peaks shown in the TIC, tentative identification of several compounds was derived, as listed in Table 6. Formation of the various low-boiling products suggests scission of the original ester alcohol group to yield 2-ethyl-1-hexanol and the hexanoic acid, as well as mixed diesters and a small amount of the adipate mono-ester at spectrum number 113. The mass spectra of the unknown products at spectrum number 201 and above all indicated the m/e 129 ion, characteristic of the adipate acyl group, and fragment ions typical of the alkyl chain of the diester parent alcohol. The distinctive diester ions of m/e 241 and 259 were absent or of low relative abundance. The products at spectrum number 213 and above all showed relatively high mass ions, of very low abundance, at m/e 469 and 470. With available information, the nature of these products can only be conjectured, possibly as oxygenated ester fragments or condensation compounds.

Due to volatility effects, the lower boiling products of oxidation were concentrated in the test condensate sample. This phenomenon is illustrated by the TIC shown in Figure 13 for the end-of-test condensate sample for Test No. 44. Probable identities of the major peaks, formulated through analysis of peak mass spectra, are described in Table 7. In addition to those products found in the sump sample, the condensate contained a measurable amount of the olefin, 2-ethyl-1-hexene, and mono-esters of acetate, propionate, and valerate. As with the sump sample, the condensate contained an insignificant amount of the adipate half-acid ester (0.1 wt percent).

GC residue data (Table 5) indicate that these high-boiling components represented the major products of oxidation. Molecular still separation of the Test No. 44 sump sample was performed to investigate the nature of the residue material. The following viscosity and acid number results compare the test sump and condensate samples with the three distillation fractions derived from the sump sample:

<u>Sample</u>	<u>100°F Vis, cs</u>	<u>Neut. No., mg KOH/g</u>
Sump	10.95	13.55
Condensate	4.28	61.0
Distillate	9.47	12.46
Residue	279.6	28.6
Cold trap	--	20.9

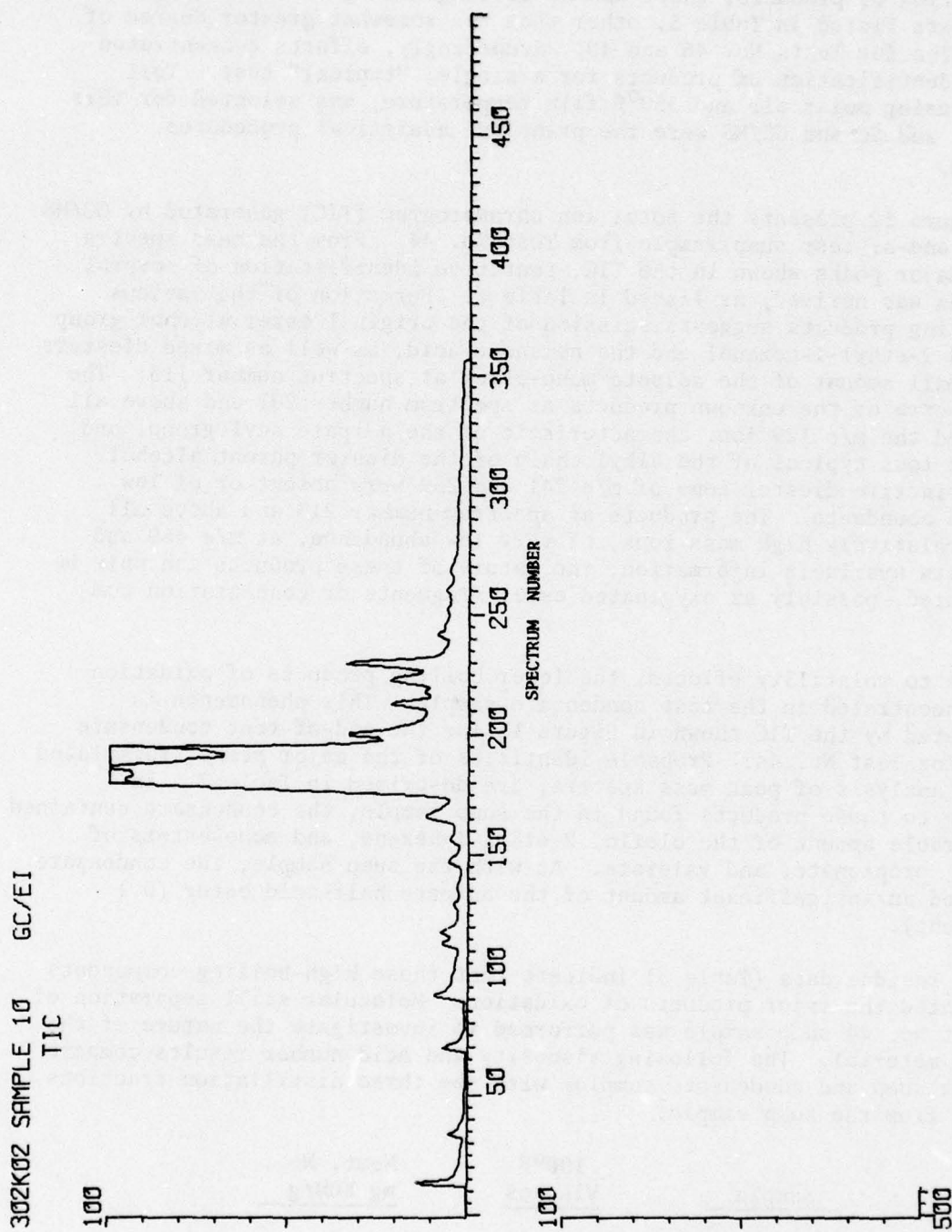


FIGURE 12. TOTAL ION CHROMATOGRAM OF TEST NO. 44 SUMP SAMPLE

TABLE 6. OXIDATION PRODUCTS IN TEST NO. 44
SUMP SAMPLE

<u>Spectrum Number*</u>	<u>Content by GC, wt %</u>	<u>Probable Compound</u>
14	0.4	2-ethyl-1-hexanol
34	0.3	2-ethyl-1-hexanoic acid
70	0.2	Unknown
92	0.9	2-ethylhexyl methyl adipate
113	0.3	2-ethylhexyl hydrogen adipate
166	0.9	Unknown
185**	66.1	di(2-ethylhexyl) adipate
201	0.9	Unknown
213	0.4	Unknown
223	0.8	Unknown
230	1.0	Unknown

* Refer to Figure 12.

** Original diester.

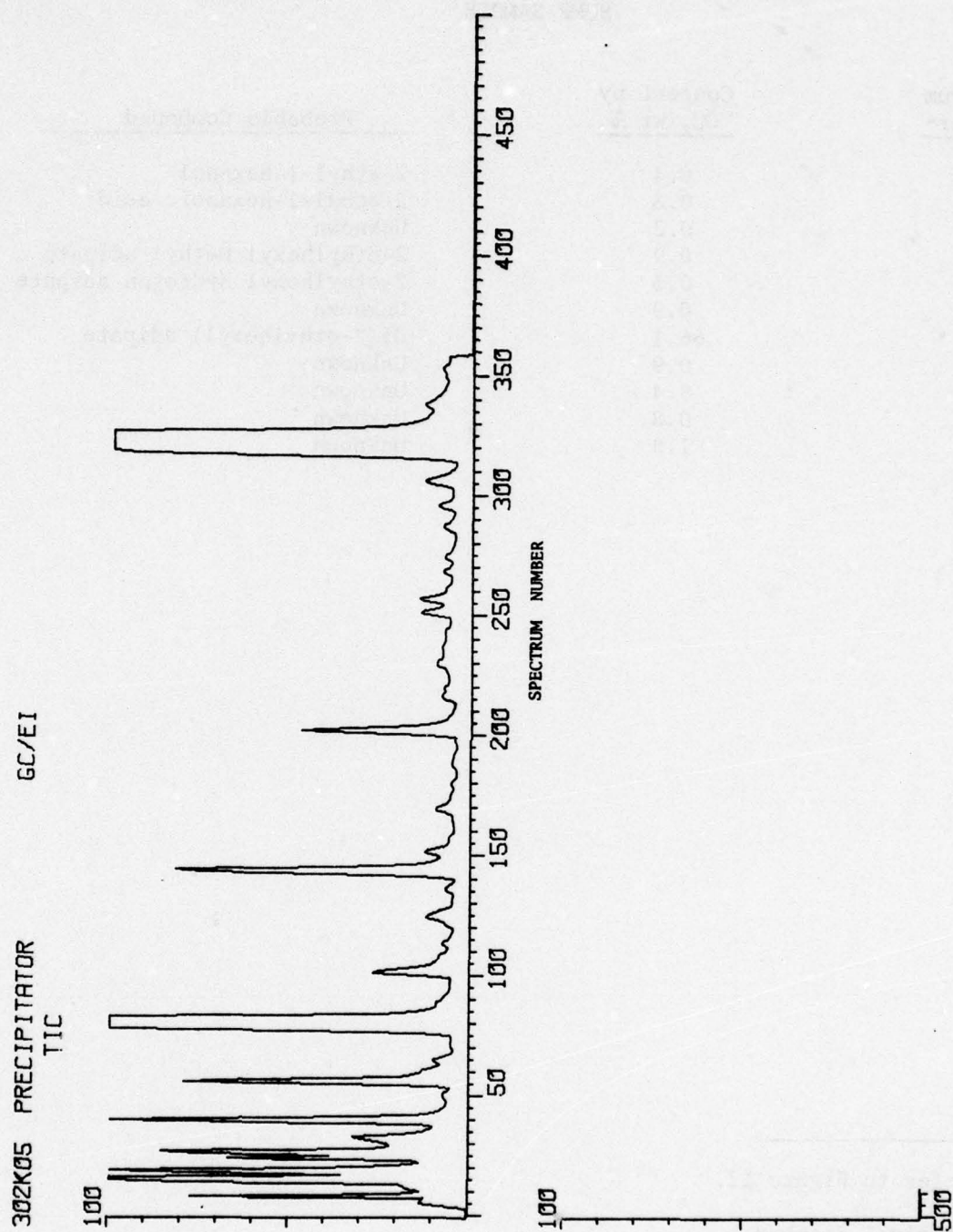


FIGURE 13. TOTAL ION CHROMATOGRAM OF TEST NO. 44 CONDENSATE SAMPLE

TABLE 7. OXIDATION PRODUCTS IN TEST NO. 44
CONDENSATE SAMPLE

<u>Spectrum Number*</u>	<u>Content by GC, wt %</u>	<u>Probable Compound</u>
8	2.2	2-ethyl-1-hexene
14	16.9	2-ethyl-1-hexanol
26	5.7	2-ethylhexyl acetate
33	1.0	2-ethyl-1-hexanoic acid
40	3.9	Unknown
56	2.8	Unknown
80	16.7	2-ethylhexyl propionate
101	1.3	Unknown
144	2.8	2-ethylhexyl valerate
202	1.4	2-ethylhexyl methyl adipate
215	0.1	2-ethylhexyl hydrogen adipate
320**	26.1	di(2-ethylhexyl) adipate

* Refer to Figure 13.

** Original diester.

The recovered still residue fraction was approximately 7 wt percent of the initial charge. The fraction indicated an exceedingly high viscosity and neutralization number. Infrared analysis was unique only with respect to a broad absorbance indicative of associated -OH in acids. The mass spectrum of the fraction, obtained by solid probe insertion, is shown in Figure 14. Ions characteristic of the original diester are evident, in addition to numerous low abundance ions in the range of m/e 150 to 275.

The presence of free adipic acid in the various oxidation test samples was not determinable because the di-acid is not eluted using an OV-17 GC liquid phase. Further, the acid is relatively insoluble in the diester, and highly volatile at the cylinder rig temperatures investigated. Thus, if formed, the compound would probably migrate to the condensing sections of the cylinder rig. This process might explain the very high acid number shown for the Test No. 44 condensate, which contained only 1 percent 2-ethyl-1-hexanoic acid but almost 17 percent 2-ethyl-1-hexanol. If present, adipic acid would be relatively soluble in the alcohol. It is also noted that the theoretical neutralization number for the amount of mono-acid found is only 4 mg KOH/g, compared with a value of 61 mg KOH/g measured for the condensate.

XRF analysis for metals gave a nil value for the intermediate and final sump samples from Test No. 44. The test condensate sample showed 100 ppm iron.

Performance Comparison for Diester and Polyol Ester Basestocks

Table 8 presents a comparison of the thermal and oxidative stability of the adipate diester versus results previously reported(1) for a trimethylol-propane triheptanoate basestock. The selected performance criteria are the critical properties of deposition and ester consumption. Due to differences in fluid capability, the results are not directly comparable with respect to test film temperature and time.

Under conditions of pyrolytic degradation, the diester basestock indicated a noticeable beneficial effect for the presence of moisture while the polyol basestock exhibited a deleterious effect for moisture, particularly with regard to increased ester consumption at the 650°F film temperature. In terms of comparative stability, the polyol ester demonstrated the superior performance relative to both deposition and ester attack. The polyester displayed a temperature capability some 25°-50°F higher than the diester for an equivalent level of thermal degradation.

Using an oxidative atmosphere, the influence of moisture in affecting ester attack was negligible for the polyester, and questionable for the diester. The 350°F data for unreacted ester in Table 8 imply some beneficial effect for moisture with the adipate ester. However, the poor repeatability of results for the three determinations using dry air does not permit a firm conclusion for the effect. While not pronounced, moisture showed some

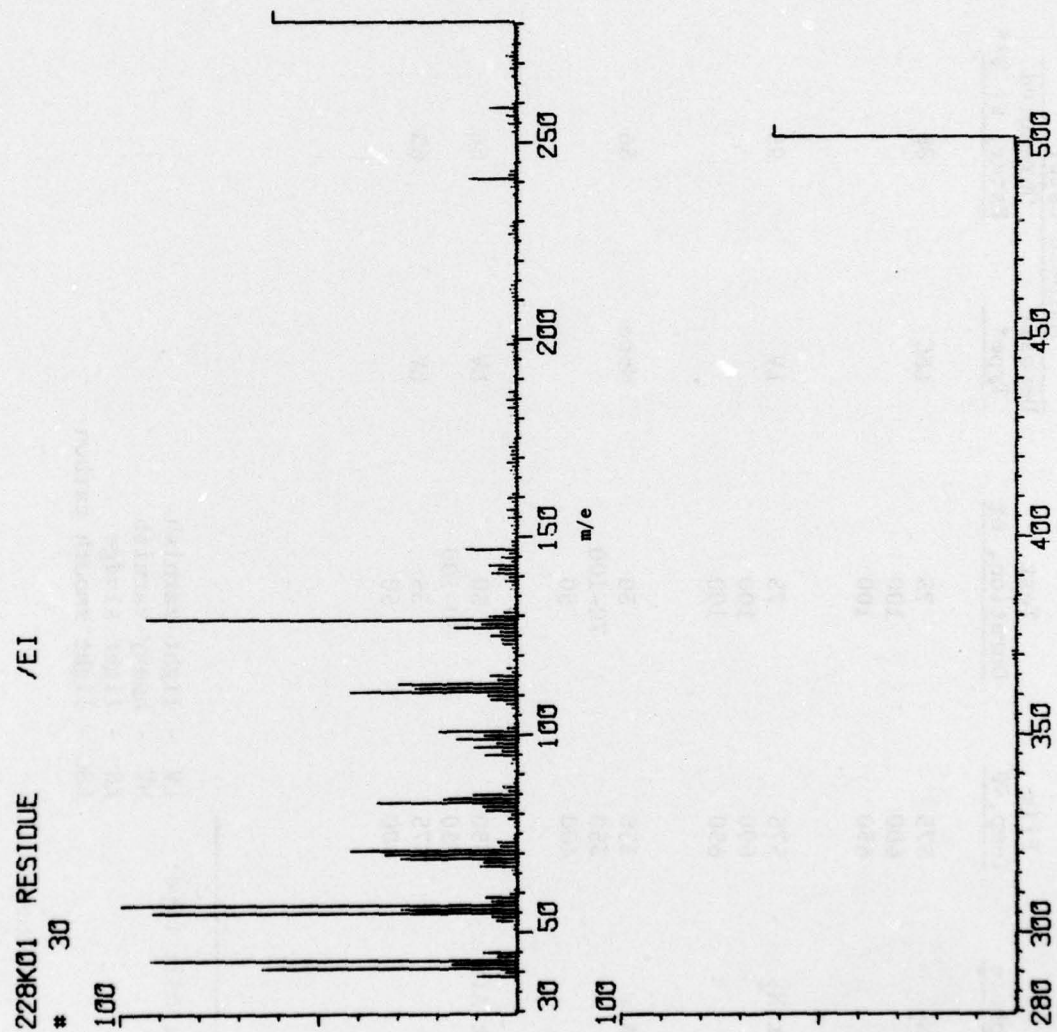


FIGURE 14. MASS SPECTRUM OF TEST NO. 44 RESIDUE SAMPLE

TABLE 8. COMPARATIVE PERFORMANCE DATA FOR DIESTER AND POLYOL ESTER BASESTOCKS

Atmosphere	Film Temp, °F	Test Duration, hr	Adipate Ester		TMP Polyol Ester	
			Deposit Type*	Unreacted Ester, wt %**	Deposit Type*	Unreacted Ester, wt %**
Dry N ₂	575	75	LSC	86	None	96
	600	100			LV	93
	650	100				
Moist N ₂	575	75	LV	95	None	94
	600	100			LV-HV	77
	650	100				
Dry Air	350	50	None	56		
	350	70-100			LV	40
	400	50			LS	42
Moist Air	350	50	LV	66		
	350	90-100			LS	45
	375	35	LV	65		
	400	50			LS	45

* Deposit type: LV - light varnish
 HV - heavy varnish
 LS - light sludge
 LSC - light smooth carbon

** Mean values.

deleterious effect with respect to deposition for both ester types. The obvious superiority of the polyester in resistance to thermal degradation was not evident for the oxidative atmosphere. Taking into account the disparities in test duration, the extent of ester consumption was virtually equivalent for the two basestocks. Furthermore, the tendency of the polyol ester to form sludge-type deposits is considered inferior to the light varnish deposition tendency of the adipate basestock.

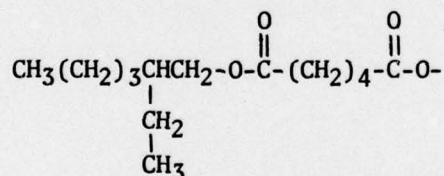
SECTION VI

CONCLUSIONS

Thin-film thermal stability experiments with an uninhibited lubricant basestock, di(2-ethylhexyl) adipate, demonstrated a significant performance effect for moisture. The effect was beneficial with respect to the degree of ester attack and deposit formation. The thermal degradation products of the diester included three low-boiling compounds characteristic of the parent alcohol of the compound, 2-ethyl-1-hexene, 2-ethyl-1-hexanol, and 2-ethyl-1-hexanoic acid. Atmospheric moisture apparently promoted formation of the acid. Molecular still separations of end-of-test samples showed a much higher viscosity and neutralization number for the moist nitrogen test residue.

A major effect for moisture was shown by deposition results for the thermal stability test series. With moisture present, an innocuous light varnish deposit occurred. Using a dry nitrogen atmosphere, significant carbon-type deposits were formed. X-ray analysis of this material showed appreciable metal contents, principally iron. Significant amounts of iron and chromium were also found in the test lubricant samples from the dry nitrogen experiment. Analysis of the carbon deposit by mass spectroscopy yielded a mass spectrum characteristic of the original diester.

The low boiling compounds resulting from thermal deterioration of the adipate ester suggest cleavage of the alcohol group. The fate of the remaining fragment of the molecule may be in the formation of condensed residue products or, in the case of the dry nitrogen tests, carbon deposits formed by metal combination compounds. A metal involvement in the deposition process seems certain. The mass spectrum of the deposit sample was virtually identical to that of the original diester. However, assuming a metal complex, the following organic moiety might exhibit a mass spectrum indistinguishable from that of the diester:



The ferrographic results provided by AFAPL showed that nascent wear particles were present in the thermal stability test samples. X-ray analysis of fluid samples indicated negligible metal amounts for the moist nitrogen determination (light varnish deposit) and significant amounts for the dry nitrogen test (carbon deposits). The source of these particles is now thought to be the rotating counterface (item 18 of Fig. 1) of the cylinder carbon seal. In more recent tests, weight measurements of this component,

constructed of AISI Type 440C stainless steel, indicated metal losses as high as 220 mg can occur. This amount would be sufficient to produce an iron content on the order of 400-500 ppm in the reduced test fluid volume at the end of a run.

With a wearmetal involvement in the deposition process, it is difficult to describe the precise role of moisture in the mechanism. Three distinct phenomena can be visualized: 1) moisture served to mitigate the wear tendency of the carbon-steel seal surfaces; 2) moisture promoted formation of a degradation product of the diester, possibly free adipic acid or 2-ethyl-1-hexanoic acid, which mitigated wear; and 3) moisture might in some way passivate the nascent wear particles to block any interaction with the diester products. The latter speculation would appear somewhat inconsistent with ferrograph data which indicated some deposit-coated metal particles present in the moist nitrogen test (Test No. 51).

With an oxidative atmosphere, cylinder rig experiments with the diester basestock did not establish a conclusive effect for moisture. At a 350°F film temperature, the poor repeatability of three tests using dry air did not permit a distinction versus the degree of deterioration in duplicate determinations using moist air. Although the amount of reacted basestock was extensive, 35-50 percent, for both oxidative conditions, the deposition tendency of the diester was insignificant. Analytical work with fluid samples from a "representative" moist air test (Test No. 44) showed numerous oxidation products in evidence. In addition to the low-boiling compounds formed by thermal degradation, the oxidation test resulted in various mixed diesters and mono-esters of C₂, C₄, and C₅ acyl groups, as well as four compounds boiling just above the original diester.

The molecular still residue fraction for Test No. 44 was highly viscous and acidic. The mass spectrum of this material showed ions generally characteristic of the adipate diester, in addition to numerous low-abundance ions.

A performance comparison between the adipate diester and a trimethylolpropane triheptanoate basestock showed a clear advantage for the polyol ester in thermal stability. Under oxidative conditions, however, there was no significant superiority for the triester with regard to basestock consumption. There was, in fact, a somewhat greater deposition tendency exhibited by the polyol ester in an oxidative atmosphere.

In the previous investigation⁽¹⁾ with the TMP polyol ester, it was also concluded that system metals played a critical role in the deposition process. It was conjectured that, in oxidative tests resulting in sludge deposits, a corrosive wear mechanism was prevalent. Findings described herein, especially ferrographic results, have demonstrated the feasibility of generating abrasive wear debris. Nevertheless, one item of data precludes modification of the corrosive wear theory in the case of the polyol ester. X-ray analysis of sludge deposit samples from the polyol ester experiments showed measurable amounts (2000 ppm) of nickel present. This

element is found in the metallurgy of several components of the cylinder rig, including the cylinder itself. Nickel is not present, however, in any of the components in rubbing contact, namely, the lubricant pump gears or body, or the seal counterface.

LIST OF REFERENCES

1. Cuellar, J. P., Jr., "Degradation Studies of a Trimethylolpropane Triheptanoate Lubricant Basestock," AFAPL Tech. Rept. 77-87, December 1977.
2. Cuellar, J. P., and Baber, B. B., "Development of a Rotating Cylinder Deposition Test," AFAPL Tech. Rept. 75-37, AD A012296, June 1975.
3. Baber, B. B., Cuellar, J. P., and Montalvo, D. A., "Deposition and Degradation Characteristics of Aircraft Turbine Engine Lubricants," AFAPL Tech. Rept. 70-8, Vol. I, AD 871991, June 1970.
4. Blum, W., "Analysis of Dicarboxylic Acid Esters (Plasticizers)," Finnigan Applications Tips, No. 42 (Munich 7), March 1972.

APPENDIX

ROTATING CYLINDER DEPOSITION TEST

SUMMARY DATA

TEST NO. 44

OXIDATIVE
ROTATING CYLINDER DEPOSITION TEST SUMMARY DATA
ON LUBRICANT O-77-1

Test Conditions

Film temp, °F 350 Lubricant-in temp, °F 350
 Film thickness, in, X 10⁻³ 4 Airflow, liters/hr 100, moist
 Lubricant flow, cm³/min 10 Lubricant charge, cm³ 1000
 Average res. time, sec/cycle 18.5 Test duration, hr 50
 Total res. time, sec 697.0

Deposit Rating

Deposit Type	Area, %	Demerits
L varnish	100	10

Overall Rating: 10

Test Lubricant Performance

Test Time, hr	100°F Vis, cs	100°F Vis Increase, %	NN Change, mg KOH/g	Unreacted Ester, wt %	Oxygen Consumption, l. at Opt
0	8.19	-	0.03	100	0
5	8.27	1.0	0.30	96.5	0.82
10	8.51	3.9	1.54	93.1	2.84
15	8.73	6.6	2.62	89.2	5.32
20	8.89	8.5	3.92	88.5	7.51
25	9.12	11.4	5.29	88.3	9.67
30	9.32	13.8	6.54	86.8	11.90
35	9.64	17.7	8.55	80.6	14.16
40	9.96	21.6	10.38	75.1	16.24
45	10.29	25.6	11.52	71.2	18.32
50	10.95	33.7	13.52	66.3	21.56

Oil loss, cm³/hr 4.8

TEST NO. 45

OXIDATIVE
ROTATING CYLINDER DEPOSITION TEST SUMMARY DATA
ON LUBRICANT O-77-1

Test Conditions

Film temp, °F 350 Lubricant-in temp, °F 350
 Film thickness, in, X 10⁻³ 4 Airflow, liters/hr 100, moist
 Lubricant flow, cm³/min 10 Lubricant charge, cm³ 1000
 Average res. time, sec/cycle 18.5 Test duration, hr 50
 Total res. time, sec 613.5

Deposit Rating

Deposit Type	Area, %	Demerits
L varnish	100	10

Overall Rating: 10

Test Lubricant Performance

Test Time, hr	100°F Vis, cs	100°F Vis Increase, %	NN Change, mg KOH/g	Unreacted Ester, wt %	Oxygen Consumption, l. at Opt
0	8.19	-	0.03	100	0
5	8.29	1.2	0.30	96.2	1.12
10	8.44	3.1	0.81	94.7	2.34
15	8.60	5.0	1.52	91.0	4.01
20	8.78	7.2	2.75	87.7	5.96
25	9.07	10.7	4.90	83.9	8.70
30	9.31	13.7	6.96	79.9	11.71
35	9.67	18.1	8.83	73.9	14.38
40	10.06	22.8	10.51	70.6	17.44
45	10.58	29.2	13.26	67.3	20.49
50	10.96	33.8	15.40	64.8	23.44

Oil loss, cm³/hr 1.8

TEST NO. 46

OXIDATIVE
ROTATING CYLINDER DEPOSITION TEST SUMMARY DATA
ON LUBRICANT O-77-1

Test Conditions

Film temp, °F	350	Lubricant-in temp, °F	350
Film thickness, in, X 10 ⁻³	4	Airflow, liters/hr	100, dry
Lubricant flow, cm ³ /min	10	Lubricant charge, cm ³	1000
Average res. time, sec/cycle	18.5	Test duration, hr	50
Total res. time, sec	622.4		

Deposit Rating

Deposit Type	Area, %	Demerits
Clean	100	0

48

Overall Rating: 0

Test Lubricant Performance

Test Time, hr	100°F Vis, cs	100°F Vis Increase, %	NN Change, mg KOH/g	Unreacted Ester, wt %	Oxygen Consumption, l at OPT
0	8.19	-	0.03	100	0
5	8.58	4.8	1.17	92.1	2.60
10	9.01	10.0	3.03	88.2	6.30
15	9.37	14.4	4.90	80.3	10.18
20	9.75	19.0	7.41	75.2	13.72
25	10.21	24.7	10.15	69.8	17.74
30	10.76	31.4	12.49	64.7	21.86
35	11.40	39.2	15.85	60.0	25.78
40	11.98	46.3	18.75	56.4	29.92
45	12.73	55.4	22.55	52.3	33.92
50	13.46	64.3	23.48	50.7	37.88

Oil loss, cm³/hr 2.7

TEST NO. 47

OXIDATIVE
ROTATING CYLINDER DEPOSITION TEST SUMMARY DATA
ON LUBRICANT O-77-1

Test Conditions

Film temp, °F	350	Lubricant-in temp, °F	350
Film thickness, in, X 10 ⁻³	4	Airflow, liters/hr	100, dry
Lubricant flow, cm ³ /min	10	Lubricant charge, cm ³	1000
Average res. time, sec/cycle	18.5	Test duration, hr	50
Total res. time, sec	670.3		

Deposit Rating

Deposit Type	Area, %	Demerits
Clean	100	0

Overall Rating: 0

Test Lubricant Performance

Test Time, hr	100°F Vis, cs	100°F Vis Increase, %	NN Change, mg KOH/g	Unreacted Ester, wt %	Oxygen Consumption, l at OPT
0	8.19	-	0.03	100	0
5	8.32	1.6	0.48	96.0	1.20
10	8.49	3.7	1.18	91.7	2.50
15	8.73	6.6	2.02	89.6	4.21
20	8.90	8.7	2.95	86.9	6.02
25	9.17	12.0	4.38	84.2	8.20
30	9.46	15.5	6.00	82.9	10.44
35	9.77	19.3	8.17	80.7	12.38
40	10.05	22.7	10.01	77.0	14.56
45	10.41	27.1	11.37	71.2	16.34
50	10.72	30.9	13.52	64.3	18.56

Oil loss, cm³/hr 4.5

TEST NO. 48

 OXIDATIVE
 ROTATING CYLINDER DEPOSITION TEST SUMMARY DATA
 ON LUBRICANT O-77-1

Test Conditions

Film temp, °F 350 Lubricant-in temp, °F 350
 Film thickness, in, $\times 10^{-3}$ 4 Airflow, liters/hr 100, dry
 Lubricant flow, cm^3/min 10 Lubricant charge, cm^3 1000
 Average res. time, sec/cycle 18.5 Test duration, hr 50
 Total res. time, sec 674.4

Deposit Type		Deposit Rating	
		Area, $\%$	Demerits
Clean		100	0

Overall Rating: 0

Test Lubricant Performance

Test Time, hr	100°F Vis, cs	100°F Vis Increase, $\%$	NN Change, mg KOH/g	Unreacted Ester, wt %	Oxygen Consumption, % at OPT
0	8.19	--	0.03	100	0
5	8.48	3.5	0.82	92.1	1.80
10	8.85	8.1	2.25	90.3	4.60
15	9.23	12.7	4.10	82.8	7.89
20	9.60	17.2	6.11	78.7	10.80
25	10.02	22.3	9.07	74.2	14.11
30	10.46	27.7	11.32	71.6	17.27
35	10.85	32.5	14.00	68.2	20.20
40	11.43	39.6	16.64	60.0	23.59
45	12.00	46.5	19.08	56.4	27.00
50	12.66	54.6	22.04	53.0	30.36

Oil loss, cm^3/hr 2.7

TEST NO. 49

 THERMAL STABILITY
 ROTATING CYLINDER DEPOSITION TEST SUMMARY DATA
 ON LUBRICANT O-77-1

Test Conditions

Film temp, °F 575 Lubricant-in temp, °F 575
 Film thickness, in, $\times 10^{-3}$ 4 Nitrogen blanket dry
 Lubricant flow, cm^3/min 10 Lubricant charge, cm^3 1000
 Average res. time, sec/cycle 16.9 Test duration, hr 75
 Total res. time, sec 926.2

Deposit Type		Deposit Rating	
		Area, $\%$	Demerits
L smooth carbon		95	85.5
M flaked carbon		5	9.5

Overall Rating: 95

Test Lubricant Performance

Test Time, hr	100°F Vis, cs	100°F Vis Increase, $\%$	210°F Vis, cs	NN Change, mg KOH/g	Unreacted Ester, wt %
0	8.19	--	2.37	0.03	100
5	8.21	0.2	2.37	0.52	97.4
10	8.22	0.4	2.37	0.75	96.2
15	8.23	0.5	2.37	0.77	95.1
20	8.16	-0.4	2.36	0.77	95.0
25	8.19	0.0	2.36	0.66	93.5
30	8.18	-0.1	2.35	0.57	92.2
35	8.15	-0.5	2.36	0.55	91.3
40	8.13	-0.7	2.35	0.51	89.5
45	8.16	-0.4	2.35	0.46	88.2
50	8.13	-0.7	2.34	0.46	87.3
55	8.17	-0.2	2.35	0.48	85.2
60	8.16	-0.4	2.34	0.51	84.5
65	8.13	-0.7	2.34	0.52	84.4
70	8.09	-1.2	2.33	0.57	83.2
75	8.13	-0.7	2.34	0.62	83.0

Oil loss, cm^3/hr 2.3

TEST NO. 50

ROTATING CYLINDER DEPOSITION TEST SUMMARY DATA
ON LUBRICANT O-77-1

ROTATING CYLINDER DEPOSITION TEST SUMMARY DATA
ON LUBRICANT O-77-1

Test Conditions

Film temp, °F 575 Lubricant-in temp, °F 575
Film thickness, in, X 10⁻³ 4 Nitrogen blanket dry 575
Lubricant flow, cm³/min 10 Lubricant charge, cm³ 1000
Average res. time, sec/cycle 16.9 Test duration, hr 75
Total res. time, sec 903.8

Film temp, °F 575 Lubricant-in temp, °F 575
Film thickness, in, X 10⁻³ 4 Nitrogen blanket moist
Lubricant flow, cm³/min 10 Lubricant charge, cm³ 1000
Average res. time, sec/cycle 16.9 Test duration, hr 75
Total res. time, sec 901.8

Deposit Rating

Deposit Type	Area, μ	Demerits
L smooth carbon	100	90

Deposit Rating

Deposit Type	Area, μ	Demerits
L varnish	100	10

Overall Rating: 90

Overall Rating: 10

50

Test Lubricant Performance

Test Time, hr	100°F Vis, cs	100°F Vis Increase, μ	210°F Vis, cs	NN Change, mg KOH/g	Unreacted Ester, wt %
0	8.19	-	2.37	0.03	100
5	8.19	0.0	2.36	0.47	96.9
10	8.22	0.4	2.36	0.78	95.0
15	8.20	0.1	2.37	0.85	95.1
20	8.20	0.1	2.37	0.95	95.1
25	8.19	0.0	2.35	0.93	94.4
30	8.17	-0.2	2.36	0.89	94.5
35	8.16	-0.4	2.36	0.84	92.4
40	8.10	-1.1	2.33	0.73	90.0
45	8.05	-1.7	2.33	0.65	88.7
50	8.05	-1.7	2.33	0.77	88.7
55	8.04	-1.8	2.32	0.91	89.0
60	7.99	-2.4	2.32	1.03	89.0
65	8.00	-2.3	2.31	1.15	88.1
70	7.98	-2.6	2.31	1.37	87.9
75	8.00	-2.3	2.32	1.54	87.9

Oil loss, cm³/hr 2.0Oil loss, cm³/hr 2.0

Test Lubricant Performance

Test Time, hr	100°F Vis, cs	100°F Vis Increase, μ	210°F Vis, cs	NN Change, mg KOH/g	Unreacted Ester, wt %
0	8.19	-	2.37	0.03	100
5	8.19	0.0	2.36	0.42	100
10	8.19	0.0	2.36	0.75	99.7
15	8.22	0.4	2.36	1.11	98.8
20	8.24	0.6	2.36	1.42	98.4
25	8.22	0.4	2.38	1.84	98.1
30	8.23	0.5	2.37	2.28	97.3
35	8.28	1.1	2.37	2.61	97.3
40	8.28	1.1	2.38	2.96	97.1
45	8.30	1.3	2.38	3.26	96.2
50	8.34	1.8	2.38	3.65	95.6
55	8.35	2.0	2.38	4.04	95.6
60	8.38	2.3	2.38	4.35	94.8
65	8.38	2.3	2.39	4.71	95.0
70	8.38	2.3	2.39	4.99	95.2
75	8.38	2.3	2.39	5.33	95.3

TEST NO. 52

THERMAL STABILITY
ROTATING CYLINDER DEPOSITION TEST SUMMARY DATA
ON LUBRICANT O-77-1

Test Conditions

Film temp, °F 575 Lubricant-in temp, °F 575
 Film thickness, in, X 10⁻³ 4 Nitrogen blanket moist
 Lubricant flow, cm³/min 10 Lubricant charge, cm³ 1000
 Average res. time, sec/cycle 16.9 Test duration, hr 75
 Total res. time, sec 896.9

Deposit Rating

Deposit Type	Area, %	Demerits
L varnish	100	10

Overall Rating: 10

51

Test Lubricant Performance

Test Time, hr	100°F Vis, cs	100°F Vis Increase, %	210°F Vis, cs	NN Change, mg KOH/g	Unreacted Ester, wt %
0	8.19	-	2.37	0.03	100
5	8.20	0.1	2.35	0.47	98.8
10	8.19	0.0	2.36	0.87	98.3
15	8.20	0.1	2.37	1.24	98.0
20	8.23	0.5	2.38	1.71	97.8
25	8.20	0.1	2.37	2.26	97.3
30	8.24	0.6	2.38	2.57	97.0
35	8.24	0.6	2.37	2.98	96.8
40	8.27	1.0	2.37	3.29	96.7
45	8.30	1.3	2.38	3.71	96.4
50	8.31	1.5	2.39	4.13	95.9
55	8.33	1.7	2.39	4.46	96.1
60	8.35	2.0	2.39	4.82	95.8
65	8.35	2.0	2.39	5.05	95.3
70	8.38	2.4	2.39	5.16	95.2
75	8.39	2.4	2.39	5.27	95.2

Oil loss, cm³/hr 2.1

TEST NO. 53

OXIDATIVE
ROTATING CYLINDER DEPOSITION TEST SUMMARY DATA
ON LUBRICANT O-77-1

Test Conditions

Film temp, °F 375 Lubricant-in temp, °F 375
 Film thickness, in, X 10⁻³ 4 Airflow, liters/hr 100, moist
 Lubricant flow, cm³/min 10 Lubricant charge, cm³ 1000
 Average res. time, sec/cycle 18.3 Test duration, hr 35
 Total res. time, sec 458.9

Deposit Rating

Deposit Type	Area, %	Demerits
L varnish	100	10

Overall Rating: 10

Test Lubricant Performance

Test Time, hr	100°F Vis, cs	100°F Vis Increase, %	NN Change, mg KOH/g	Unreacted Ester, wt %	Oxygen Consumption, % at O.P.T.
0	8.19	-	0.03	100	0
5	8.46	3.3	1.15	94.3	2.13
10	8.79	7.3	2.74	90.3	5.28
15	9.15	11.7	4.55	84.9	8.54
20	9.41	14.9	7.34	81.8	11.90
25	9.96	21.6	9.74	77.0	16.00
30	10.57	29.1	12.80	69.1	20.38
35	11.42	39.4	14.09	65.1	25.14

Oil loss, cm³/hr 3.4

TEST NO. 54

OXIDATIVE
ROTATING CYLINDER DEPOSITION TEST SUMMARY DATA
ON LUBRICANT O-77-1

Test Conditions

Film temp, °F 375 Lubricant-in temp, °F 375
Film thickness, in; $\times 10^{-3}$ 4 Airflow, liters/hr 100, moist
Lubricant flow, cm³/min 10 Lubricant charge, cm³ 1000
Average res. time, sec/cycle 18.3 Test duration, hr 35
Total res. time, sec 429.0

Deposit Rating

Deposit Type	Area, %	Demerits
L varnish	100	10

Overall Rating: 10

Test Lubricant Performance

Test Time, hr	100°F Vis, cs	100°F Vis Increase, %	NN Change, mg KOH/g	Unreacted Ester, wt %	Oxygen Consumption, l at OPT
0	8.19	-	0.03	100	0
5	8.46	3.3	1.38	92.9	2.82
10	8.77	7.1	3.13	90.2	6.40
15	9.16	11.8	5.05	85.6	10.05
20	9.56	16.7	7.06	81.9	14.23
25	10.07	23.0	9.57	75.9	18.74
30	10.71	30.8	11.46	71.1	23.44
35	11.45	39.8	13.35	65.7	28.04

Oil loss, cm³/hr 4.3

ED
78